



Final validation report

Deliverable No: 5.5

Ref.: WP5

Date: April 2017



This project has received funding from the European Union's Seventh Framework Programme for research, technological development and demonstration under grant agreement n° 607131.

Grant Agreement number: **607131** / Project acronym: **FAST**
Project title: **Foreshore Assessment using Space Technology**
Funding Scheme: **Collaborative project** / Project start: **01-01-2014**
Project duration: **48 months** / Project coordination: **Deltares, Delft, the Netherlands**
Project website: **fast-space-project.eu** / DG Research - FP7 - SPACE - 2013

Deliverable Title	D.5.5 – Final validation report
Filename	FAST_D.5.5_Final validation report_v0.1
Authors	Gerrit Hendriksen (Deltares) Jasper Dijkstra (Deltares) Joan Sala Calero (Deltares) Kees Nederhoff (Deltares) Edward Morris (UCA) Iris Möller (UCam) Daphne van der Wal (NIOZ)
Contributors	Myra van der Meulen (Deltares) Mindert de Vries (Deltares) Annette Wielemaker (NIOZ) Bas Oteman (NIOZ)
Date	20/04/2017

Dissemination level		
<input checked="" type="checkbox"/>	PU	Public
<input type="checkbox"/>	PP	Restricted to other programme participants (including the Commission Services)
<input type="checkbox"/>	RE	Restricted to a group specified by the consortium (including the Commission Services)
<input type="checkbox"/>	CO	Confidential, only for members of the consortium (including the Commission Services)

Document Change Record

Authors	Modification	Issue	Date
MdV, KN, JSC, GH, MvdM	v0.2	Restructuring of outline	18/04/2017
MdV, KN, JSC, GH, MvdM	v0.3	First draft	20/04/2017
KN, JSC, GH, MvdM, DvdW, IM	V0.4	Final draft	25/04/2017
MdV, MvdM	V1.0	Final version	30/04/2017



Content

Executive summary / Abstract	4
Scope	5
1 Introduction	6
2 Inputs	9
2.1 Hydraulic boundary conditions: water levels and wave heights	9
2.2 Bathymetry	10
2.3 Intertidal elevation	12
2.4 Topography	18
2.5 Vegetation absence/presence	18
2.6 Vegetation type	19
2.7 Vegetation biophysical parameters: NDVI	21
3 Output	24
3.1 Model description	24
3.2 Calibration of output	25
3.3 Model inaccuracies	31
3.4 Challenges	33
4 References	37
Annex I: Example metadata files	39



Executive summary / Abstract

The objective of the FAST project is to develop Copernicus downstream services. The role of work package 5 (WP5) is to develop the MI-SAFE package, as well as developing the business case and the interaction with end users. The project has implemented several products and services, including an online viewer 'MI-SAFE', a wealth of downloadable data layers, Open Software modelling and more Advanced services (training and consultancy). Together, we call this the 'MI-SAFE package', which is available online via this link: <http://fast.openearth.eu/index.htm>. In this deliverable we focus on the validation and uncertainty in the Earth Observation (EO) and field data used as input into the XBeach modelling calculations as well as on the quality of the outputs from the model.



Scope

The EU Foreshore Assessment using Space Technology (FAST) project focuses on the assessment of foreshores, including vegetation and stability variables, using satellite imagery, to be used in a foreshore assessment package, named MI-SAFE. This report, Deliverable 5.5 (D5.5), describes the validation of the inputs and outputs of the XBeach model calculations as well as discussing the challenges associated with the Educational and Expert modalities of the MI-SAFE viewer.



1 Introduction

The FAST project aims to develop Earth Observation (EO)-based downstream services that facilitate the use of foreshores a part of nature based flood defences. Part of these services are to use model calculations with the open source model XBeach (<https://oss.deltares.nl/web/xbeach/>) and translate outputs into changes in crest height of sea defences as a result of wave attenuation by foreshore vegetation. These outputs provide an indication of the importance of foreshore areas in flood defence strategies and can aid managers and policy makers in understanding the principles of nature based flood defence as well as in quantifying these characteristics for design and discussion purposes.

Throughout the FAST project, Earth Observation (EO) products (Leaf Area Index/Normalized Differentiated Vegetation Index) were used to assess foreshore areas and their vegetation, and EO products were combined with measurements from field measurements in the 8 case study areas (UK: Tillingham, Donna Nook; NL: Paulina, Zuidgors; RO: Jurilovca, Histria; ES: two locations in the Bay of Cadiz).

In previous deliverables we have discussed the results from the final end user consultation on the MI-SAFE package (D5.8) and the release of the MI-SAFE functional prototype (D5.12). Both documents are publically available through the FAST website (<http://www.fast-space-project.eu/index.php/results/public-deliverables>). In these deliverables we described the data sources, products and model calculations used as building blocks for the MI-SAFE viewer and its outputs. In the current deliverable, the focus will be on the validation of the input and output of the model calculations made with XBeach. Here, we will discuss the uncertainties and inaccuracies in the input data from global datasets, EO and the field measurements as well as the threshold values used to, for example, classify vegetation into different groups. A short discussion on the uncertainties in the XBeach model itself as well as the challenges that the outputs of the MI-SAFE viewer still poses for specific environments, is included.

The general idea behind the FAST service is to combine the best data sources available for the given selection made by end users of the MI-SAFE viewer. The following work flow (Figure 1.1) describes how data is retrieved and all the assumptions involved in the process, it has been divided into 5 steps:



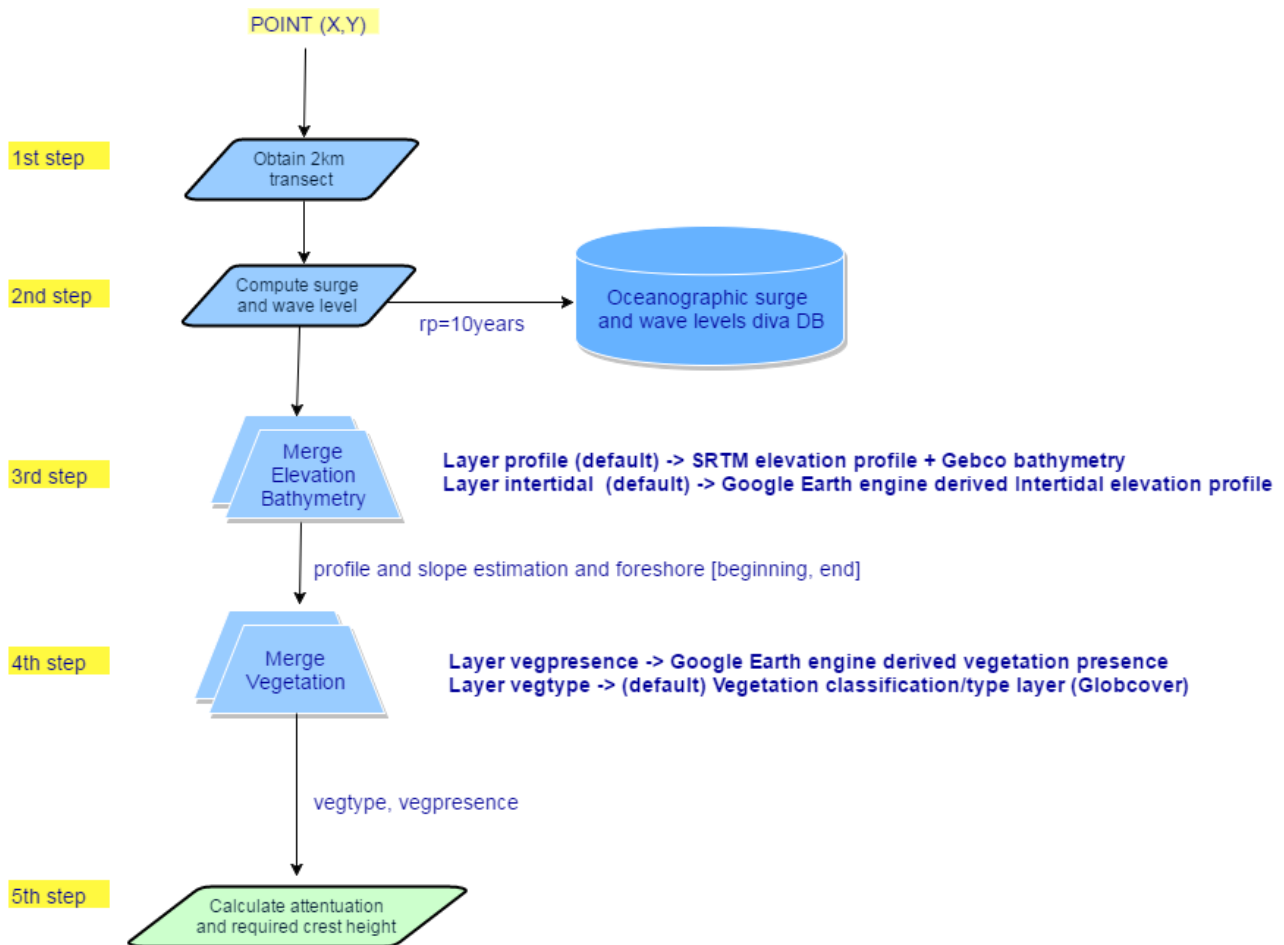


Figure 1.1 Work flow used in MI-SAFE viewer.

1st step: Obtain a 2km transect perpendicular to the closest shore according to the OpenStreepMap coastlines dataset.

2nd step: Query the surge and water levels database (pre-calculated DIVA values, <http://www.diva-model.net/>) for the given location. A storm event return period of 10 years is selected (rp=10years). This should be understood as an event that has a likelihood of 10 % for occurring in any given year.

3rd step: Get the transect elevation values taking into account 3 sources (GEBCO for bathymetry, SRTM for topography and the Google Earth Engine intertidal elevation map). Those 3 datasets overlap and priority is given by the following rule Intertidal > SRTM > GEBCO. In the following example transect the three sources are merged with the mentioned rule (Figure 1.2):



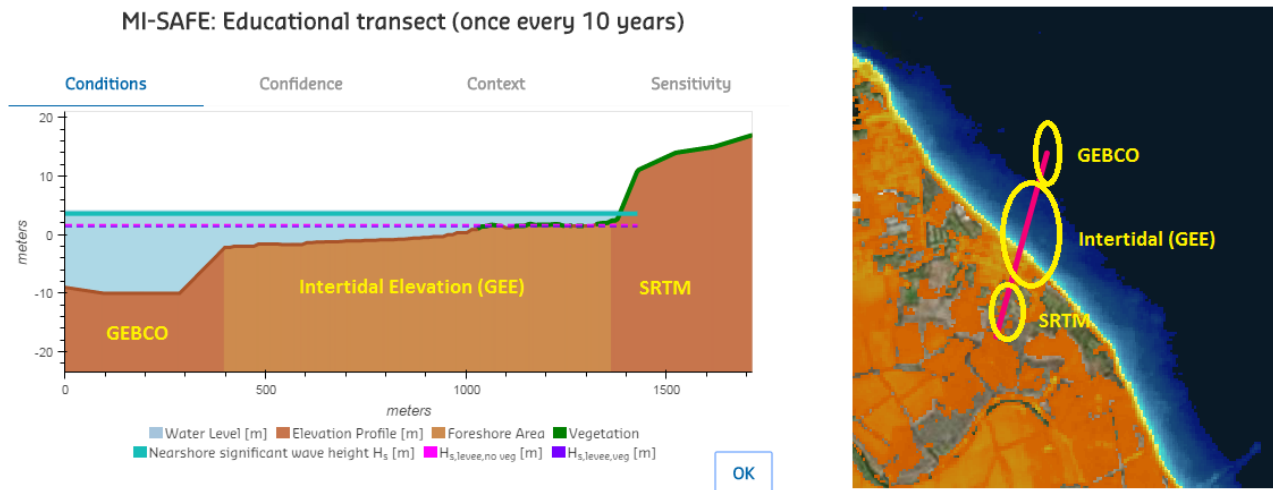


Figure 1.2 Picture demonstrating how the different data layers are combined to provide a result in the MI-SAFE viewer.

4th step: Get the vegetation presence and type for the selected transect. That is done by querying the Google Earth Engine (GEE) vegetation presence layer and the Globcover reclassification layers for the foreshore area estimated in the 3th step. That area corresponds to the beginning of the intertidal until it matches the surge level from step 2. Produce depth-limited nearshore wave height at the seaward end of the transect.

5th step: In the last step the context information such as required crest height with and without vegetation and attenuation coefficients are sent back to the web interface.



2 Inputs

2.1 Hydraulic boundary conditions: water levels and wave heights

Wave attenuation over foreshores is typically most relevant during storm conditions that create a surge (water level set-up), in combination with high tides and high wave heights. For hydraulic boundary conditions, two datasets have been used:

1. Global Tide and Surge Model (GTSM, Muis et al., 2016, see Figure 2.1): for extreme water levels (tide + atmospheric-driven surge);
2. ERA-Interim for offshore wave heights and periods.

URL: <http://www.ecmwf.int/en/research/climate-reanalysis/era-interim>

GTSM has a nearshore resolution of ~5 km and provides data on coastal (DIVA) segments that requires no further transformation. However, validation of the model results showed that the extreme sea levels are slightly underestimated due to coarse resolution of the meteorological forcing (<0.45 m for 90% of the observation stations).

In contrast, the ERA-Interim data comes on a 0.75° grid, meaning that information is usually only available several 10's of kilometres offshore. The translation of an offshore wave height to a nearshore wave height occurs via a simple depth-limiting criterion that works reasonably well for exposed coasts but may fail in sheltered areas. However, no extended validation of the extreme wave conditions was carried out.

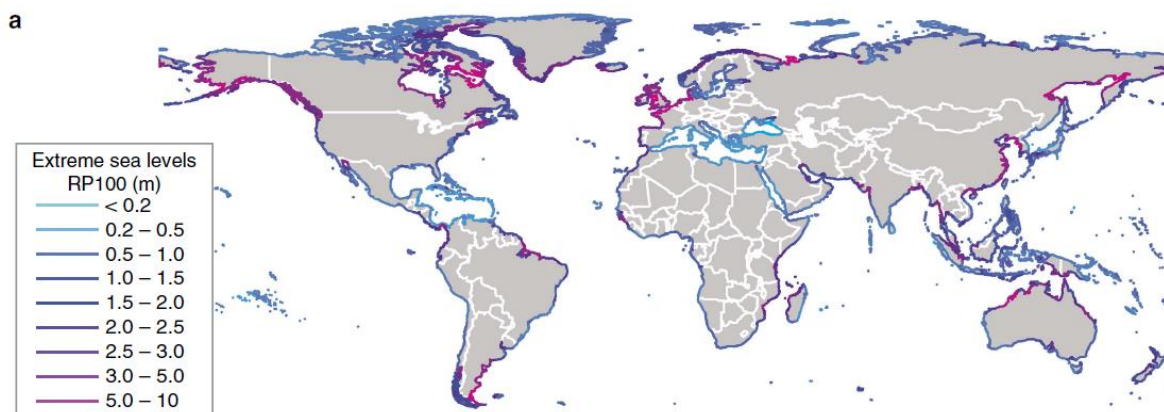


Figure 2.1 Global extreme water levels (tide + surge) for a return period of 100 years. From Muis et al. (2016).

2.1.1 Educational mode

Because there is no data on relevant return periods, all global assessments are based on conditions that individually have a 1 in 10 years return period. This represents a storm that both occurs often enough to appeal to the user and is high enough to be a serious threat to coastal regions.



2.1.2 Expert mode

For the Expert version of MI-SAFE, also boundary conditions for 1/100 and 1/1000 year conditions are used, to display the effects of more severe (for economically developed areas more appropriate) conditions on flood risk reduction. If available, site-specific boundary conditions can also be used and the direction of the waves can be included.

2.2 Bathymetry

2.2.1 Educational mode

In the Educational version, the depth information was obtained from the GEBCO (General Bathymetric Charts of the Ocean:

http://www.gebco.net/data_and_products/gridded_bathymetry_data/). The GEBCO's gridded bathymetric data sets are global terrain models for ocean and land, but in the MI-SAFE viewer only the ocean information is applied. GEBCO has a resolution of 1 km x 1 km and has been obtained from sources believed to be reliable, but the vertical accuracy is not known. Most likely the main coastal features are present, but local (smaller-scale) patterns will be lacking.

2.2.2 Expert mode

In the Expert version local depth information was used to estimate the bathymetry. An overview of the data source, per case study, resolution and accuracy is provided in Table 2.1.

Table 2.1 Data sources for the topography in the expert version

Case study	Source	Resolution (m)	Vertical accuracy
Tillingham, UK	EMODnet	100	Check EMODnet documentation
The Netherlands	Vaklodingen	20	0.4 m (Wiegmann <i>et al</i> 2005)
Cadiz, UK	EMODnet	100	Check EMODnet documentation
Jurilovca, RO	EMODnet	100	Check EMODnet documentation

The Expert version uses the best products for bathymetry available as Open Data. Except for the Dutch Coast there are currently only EMODNet bathymetry data incorporated from the study sites. This data is derived from several bathymetric surveys, each with their own metadata. For Tillingham site the bathymetry is built-up of several data sources which is clearly shown next figure (Figure 2.2).



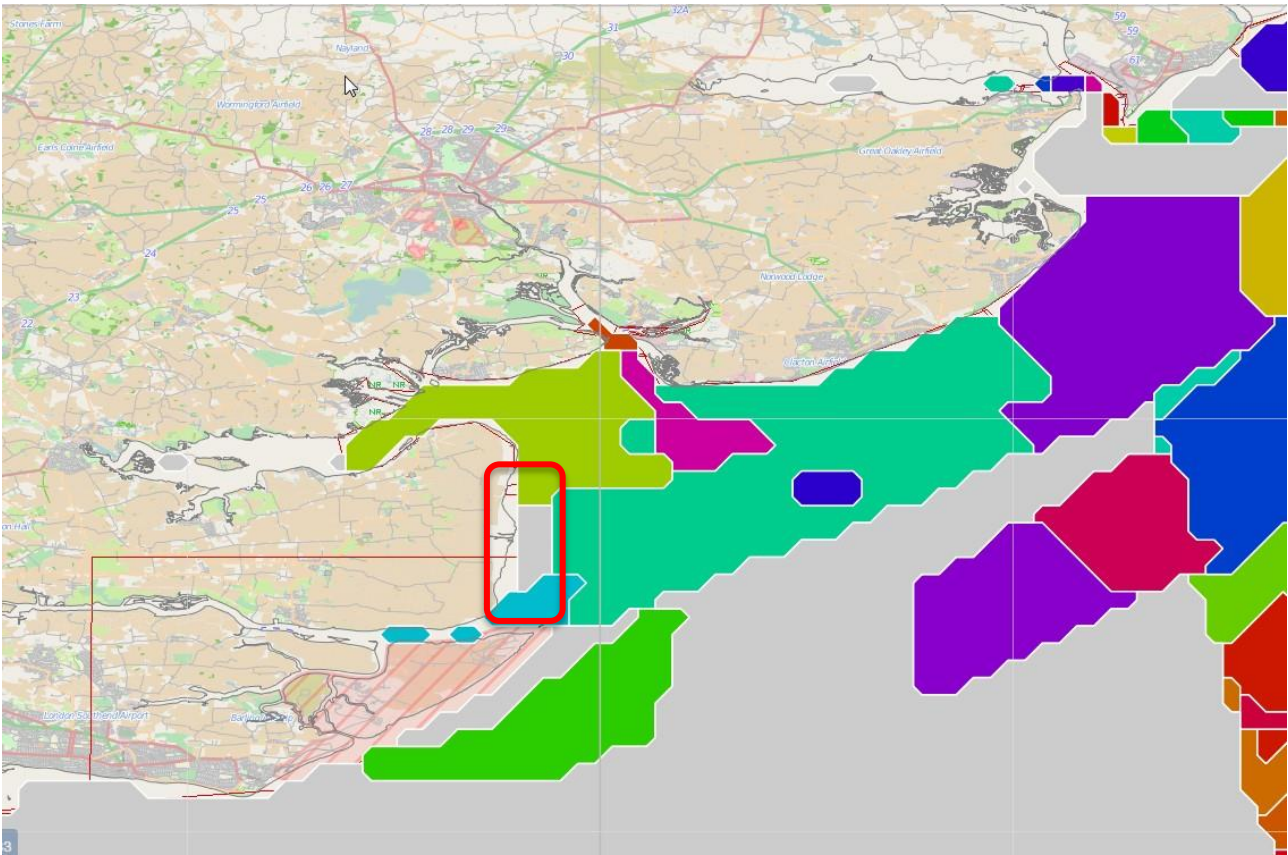


Figure 2.2 EMODnet bathymetry source references (<http://portal.emodnet-bathymetry.eu/source-references>)

The grey area just in front of Tillingham (red polygon) is interpolated from the other sources (the green colours) around it. In other words, bathymetry for Tillingham consists of single-beam echo sounders with a vertical resolution of 0.001 meter measured in the period between 1980 and 1985. Every source has its own metadata record. On the portal of EMODnet Bathymetry the origin is very well described.

For the site in Spain, Cadiz Bay, two datasets are used to construct the bathymetry. Metadata of one of these datasets is listed as an example in the Annex (Annex I: Example metadata files).

The Dutch vaklodingen dataset is a very well documented dataset. Vaklodingen dataset covers the complete coastal zone of the Netherlands. The next figure, Figure 2.3, shows an example of this for the WaddenSea area.



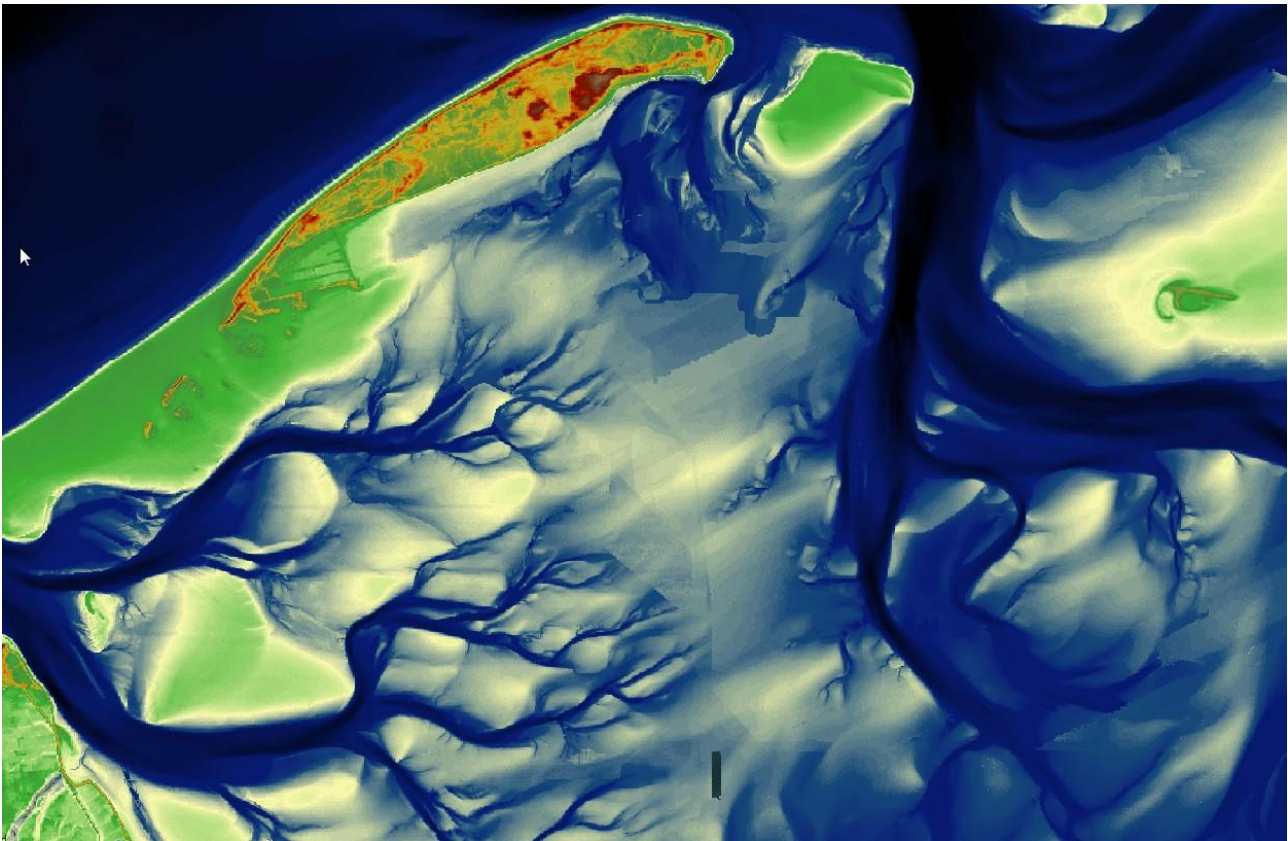


Figure 2.3 Vaklodengen combined with AHN2

On the OpenEarth page all references are listed.

<https://publicwiki.deltares.nl/display/OET/Dataset+documentation+Vaklodengen>

2.3 Intertidal elevation

2.3.1 Expert (in situ elevation datasets)

For the purpose of validation and accuracy assessment we used in situ elevation datasets collected using dGPS at each of the FAST case study sites, and high resolution digital elevation models (Table 2.2). For the UK and NL sites, OA, quality Digital Terrain Models (DTM) generated by local authorities were available. For the Spanish FAST case study sites, available DTMs were deemed unsatisfactory (they had poor coverage in inter-tidal areas) hence a Unmanned Aerial Vehicle (UAV) flight from the Univ. Cadiz central services was commissioned and a high-resolution digital surface model was derived using structure-from-motion techniques for site ES_2. Two wetland sites in the USA with quality DTMs combining multi-temporal bathymetric and lidar surveys provided by the [USGS project CoNED](#) (Danielson et al. 2016), and readily available vertical datum conversions (using the [online VDatum tool](#)) were also included.

Table 2.2. Insitu elevation data sets used in this study. Abbreviations: Foreshore Assessment using Space Technology (FAST), Univ. Cádiz (UCA), Univ. Cambridge (UCAM), Netherlands Institute for Sea Research (NIOZ), Actueel Hoogte Bestand Nederland (AHN), unmanned aerial vehicle (UAV), structure-from-motion (SfM), Coastal National Elevation Database (CoNED). Note pixel resolution is that of the original data set; digital terrain models were bilinear re-sampled to 20 m. * Vertical resolution of the multi-source CoNED data sets was not evaluated, but is assumed to be similar to standard Lidar.



Source	Provider	Name	ID	Date range	Resolution xy (m)	Resolution z (m)
FAST project	UCA	In-situ dGPS elevation	FAST_ES_1_dgps_2014-2015	2014-2015	0.02	0.02
FAST project	UCA	In-situ dGPS elevation	FAST_ES_2_dgps_2015-2016	2015-2016	0.02	0.02
FAST project	UCA	UAV SfM digital surface model	FAST_ES_2_uav-sfm-1m-epsg25829_2015-2016	2015-2016	1.00	0.02
FAST project	UCAM	In-situ dGPS elevation	FAST_UK_1_dGPS_Core_2014-2015	2014-2015	0.02	0.02
FAST project	UCAM	In-situ dGPS elevation	FAST_UK_1_dGPS_Ancillary_2014-2016	2014-2015	0.02	0.02
FAST project	UCAM	In-situ dGPS elevation	FAST_UK_2_dGPS_Core_2015-2016	2015-2016	0.02	0.02
FAST project	UCAM	In-situ dGPS elevation	FAST_UK_2_dGPS_Ancillary_2015-2016	2015-2016	0.02	0.02
FAST project	DATA.GO V.UK	Lidar composite digital terrain model	Donna Nook DTM	2009-09-26	0.50	?
FAST project	DATA.GO V.UK	Lidar composite digital terrain model	Tillingham DTM	2015-05-31	0.50	?
FAST project	NIOZ	In-situ dGPS elevation	FAST_NL_1_dGPS_Core_2014-2015	2014-2015	0.02	0.02
FAST project	NIOZ	In-situ dGPS elevation	FAST_NL_2_dgps_core	2015-2016	0.02	0.02
FAST project	NIOZ	In-situ dGPS elevation	FAST_NL_2_dgps_Transect	2015-2016	0.02	0.02
FAST project	AHN	Lidar composite digital terrain model	Netherlands_Study_Site_Paulina:DTM	2015-05-31	0.50	0.01
USGS	CoNED	Topobathymetric Digital Elevation Model (TBDEM)	Chesapeake_Topobathy_DEM_v1_56	1859 - 2015	1	~0.2*



USGS	CoNED	Topobathymetric Digital Elevation Model (TBDEM)	Northern_Gulf_of_Mexico_ Topobathy_DEM_12	1888 - 2013	3	~0.2*
----------------------	-----------------------	---	--	-------------	---	-------

2.3.2 Educational (global scale FAST intertidal product)

For use in the educational modality, the global-scale FAST intertidal product was developed. A qualitative and quantitative check of performance of the algorithm was performed.

Qualitative assessment

The initial product generation consisted of applying the intertidal elevation processing chain to the global coastline divided into ~ 25000 AOI of about 40x40 km² using the [OSM shoreline](#). This resulted in a proportion (~ 15%) of AOIs that failed during the processing. For many of these there was an obvious explanation; they tended to be AOIs with no shoreline, either offshore or inland, or areas with no LAT/HAT predictions (such as the Caspian Sea). In general the product appeared to represent plausible inter-tidal topography in a number of tidal regions. Although, visual differences between adjacent AOIs were regularly observed, highlighting potential issues with using the self-contained AOI approach (Figure 2.4).

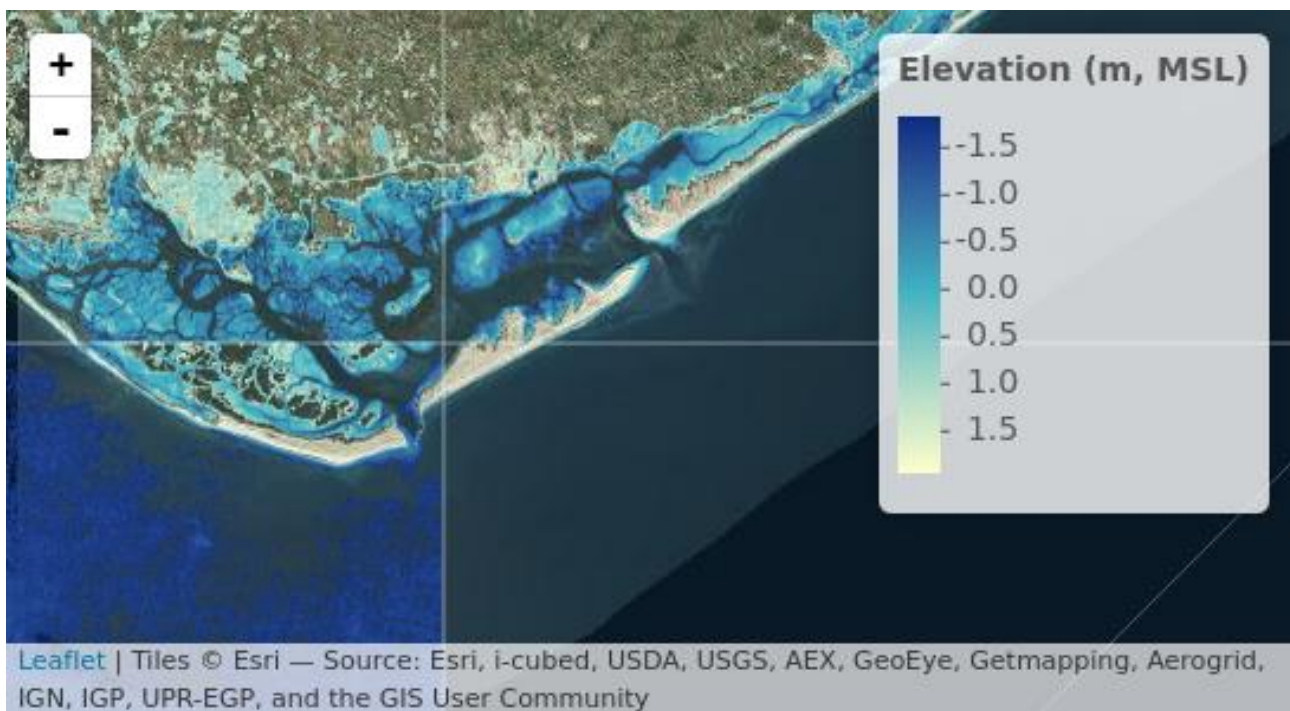


Figure 2.4. Map showing inter-tidal elevation of Ria Formosa, Portugal (AOI 164_030, 164_035 and 164_037, lat:36.98, long:-7.80).

Indeed, erroneous results were systematically observed in a range shorelines, mainly related to ‘false-positives’ in terms of identifying open water in the image collections. For example, volcanic



substrates, which have modified normalised-difference water index (MNDWI) values similar to water, resulted in the false assignment of inter-tidal elevation. The same type of effect was also caused by snow cover and shadows from terrain. Errors of omission, e.g., known tidal flats not represented by the product, were also observed, for example in the Wadden Sea, NL. Here it is not directly clear why the technique failed, although the dynamic nature of the tidal flats might be an issue.

Quantitative assessment

Quantitative validation and accuracy assessment was carried out by comparing predicted inter-tidal elevation values to in-situ data sources (Table X) using the coefficient of determination (R^2), root-mean squared error (RMSE) and mean absolute error (MAE). In-situ elevation data was supplied relative to an appropriate local vertical datum, and converted to local mean sea level (LMSL) using a specific factor for each site. For the ES, NL, UK and USA sites, this was based on a local tidal station (Cadiz III), Normaal Amsterdams Peil (NAP), Ordnance Datum Newlyn (ODN), and North American Vertical Datum of 1988 (NAVD 88), respectively.

In situ dGPS measurements from both case study sites in each country (apart from micro-tidal RO) were combined with digital terrain model (DTM) data, bi-linear re-sampled to 20 m pixels, to allow an overall comparison of the accuracy of predictions (Figure 2.5). Coefficient's of determination for a linear relationship between predicted and observed elevation at the FAST case study sites ranged from 0.45 to 0.75, suggesting a reasonable fit. Examination of the scatter plots hinted at some non-linearity in the relationship towards the extremes of the inter-tidal ranges. RMSE and MAE values, estimates of the accuracy of predictions, ranged 0.32 m to 0.92 m, suggesting predictions were generally within 1 m of the observed value. Particularly at the UK sites, which are separated by large distances, this may be improved by further adjustments of the in situ data for ODN to LMSL bias.

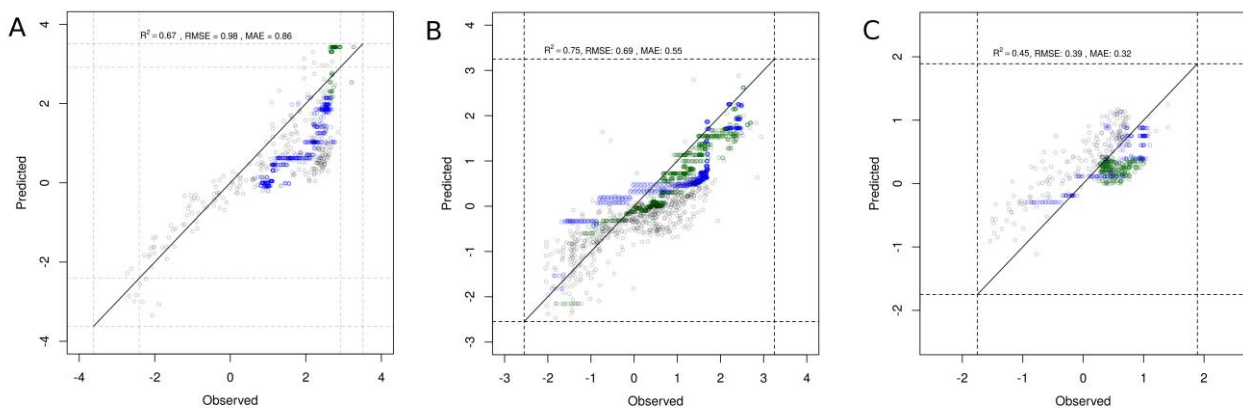


Figure 2.5. Scatterplot showing observed versus predicted inter-tidal elevation (m, LMSL) at the case study sites. A) UK_1 and UK_2 on the east coast of the UK, B) NL_1 and NL_2 in the Westerschelde, SW Netherlands, C) ES_1 and ES_2 in Cádiz Bay, SW Spain. Green and blue points represent dGPS measurements (vertical accuracy of ± 0.02 m) from case study sites 1 and 2, respectively. Grey points are data derived from a high resolution DTMs (see Table 2), bilinear re-sampled to 20m pixels. Dashed lines represent LAT and HAT values for the region. Solid line is the 1:1 relationship. Statistical measures of 'goodness-of-fit' are also shown.

As an independent validation of the global-scale FAST intertidal product, two US coastal wetland sites were selected with USGS CoDED TDEM coverage (Danielson et al. 2016). The choice of



these sites was essentially related to data availability, metadata and quality; the data sets are OA, well-documented, specifically cover the inter-tidal and vertical datum conversions are readily available.

The first test site was a section of the Atchafalaya Delta in the Atchafalaya Basin, LA, USA (Figure 2.6A). High-resolution elevation data from the CoDED TDEM product clearly shows the 'birds-foot' structure of the accreting delta (Figure 2.6B); < LMSL land-types tend to be bare sediment tidal flats, whereas >LMSL coverage tends to be dense marsh vegetation. In comparison the FAST intertidal elevation product captures the general structure of the delta (Figure 2.6C); although with less detail, and enclosed regions are missing. A direct comparison of the observed and predicted values from a selection of 10000 randomly distributed pixels suggests predictions are noisy ($R^2 = 0.21$), but reasonably accurate (RMSE = 0.44 m, MAE = 0.24 m). Examination of the scatterplot suggests that the FAST product had a bias to underestimate elevation, and that there were some regions where predicted elevation varied, but observed values were constant (vertical lines of points). Considering the active accretion at the site, and the potential differences in the observation time-periods these differences appear reasonable.

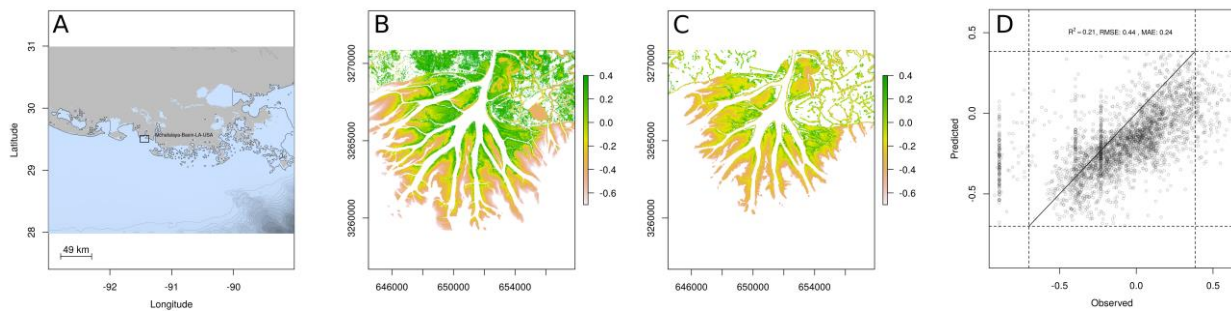


Figure 2.6. Maps and scatterplot showing observed and predicted inter-tidal elevation (m, LMSL) at the Atchafalaya Basin, LA, USA (lat:29.51, long: -91.45). A) Map showing bounding box of test region in the Northern Gulf of Mexico, B) observed elevation (m, LMSL) derived from USGS CoDED TDEM product, C) predicted elevation (m, LMSL) derived from the FAST intertidal elevation product, and D) scatterplot showing observed versus predicted inter-tidal elevation (m, LMSL). $n = 10000$ randomly selected pixels. The high resolution DTM was bilinear re-sampled to 20m pixels. Dashed lines represent LAT and HAT values for the region. Solid line is the 1:1 relationship. Statistical measures of 'goodness-of-fit' are also shown.

The second test site was situated in Virginia on the central-eastern coast of the USA, within the marshes and barrier islands, near the town of Wachapreague (Figure 2.7A). The TDEM data shows the detailed structure of the salt-marshes and tidal flats within the coastal lagoon (Figure 2.7B), and once again the FAST product captures this general distribution (Figure 2.7C). Examination of the scatterplot (Figure 2.7D) suggests, as for the first test site, scatter was high ($R^2 = 0.29$), but the prediction accuracy was reasonable (RMSE = 0.49 m, MAE = 0.35 m). Once again, the FAST product had a bias towards lower elevation and suggested there were regions that had elevation, which were not observed in the TDEM product. As before this may potentially be related to mismatches in the temporal period of the datasets.



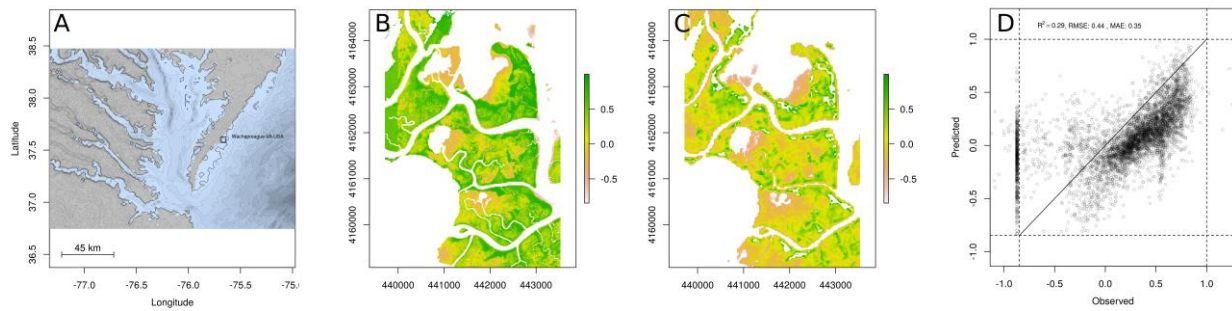


Figure 2.7. Maps and scatterplot showing observed and predicted inter-tidal elevation (m, LMSL) at the Wachapreague, VA, USA (lat:37.58, long:-75.68). A) Map showing bounding box of test region in the Chesapeake Bay coast, B) observed elevation (m, LMSL) derived from USGS CoNED TDEM product, C) predicted elevation (m, LMSL) derived from the FAST intertidal elevation product, and D) scatterplot showing observed versus predicted inter-tidal elevation (m, LMSL). $n = 10000$ randomly selected pixels. The high resolution DTM was bilinear re-sampled to 20m pixels. Dashed lines represent LAT and HAT values for the region. Solid line is the 1:1 relationship. Statistical measures of ‘goodness-of-fit’ are also shown.

Overall, the demonstration, global FAST intertidal product appears to perform relatively well at selected test sites (tidal wetlands), providing a reasonable qualitative representation of topobathymetry, and allowing predictions of elevation at 20 m horizontal resolution with a vertical accuracy of between 0.3 m and 0.9 m (RMSE). To put this level of accuracy in context, DTMs derived from Lidar often have a stated vertical accuracy of 0.2 m, whereas global DTMs (derived from radar) tend to be in the 5-20 m range. Hence, the FAST intertidal product has potential to provide enhanced intertidal elevation data in many data-scarce regions of the world, as well as guide and compliment high-resolution data collection.

Furthermore, integrating over a large temporal-period, and by definition providing information relative to LMSL in the difficult to access intertidal region, it may have a special application in efforts to produce continuous topography-bathymetry data sets (Danielson et al. 2016). We also see plenty of potential refinements of the technique (some of which should be ready for the public release in June 2017); improvement of the areas-of-interest on the global coast, automatic removal of product artifacts (urban/mountain shadows, offshore wind), inclusion of more sensors (such as Sentinel 1 C-Band SAR), conversion from surface to terrain elevation, and developing techniques to allow examination of data over shorter time-periods.



2.4 Topography

2.4.1 Educational mode

In the educational version, the topography information (elevation above Mean Sea Level, MSL) was obtained from the SRTM (Shuttle Radar Topography Mission 4.1) global elevations data sets. The SRTMs gridded data sets are global terrain models for land with a resolution of 30 m x 30 m. The performance of topography compared to ground truth based on SRTM varies per continent and region. The SRTM absolute vertical accuracy is better than 9 m (Farr et al., 2007).

2.4.2 Expert mode

In the Expert version local Digital Elevation Models (DEM) were used to estimate the topography. An overview of the data source per case study, resolution and accuracy, is provided in Table 2.3.

Table 2.3 In-situ elevation data sets used in this study. Abbreviations: Foreshore Assessment using Space Technology (FAST), Univ. Cádiz (UCA), Univ. Cambridge (UCAM), Netherlands Institute for Sea Research (NIOZ), Actueel Hoogte Bestand Nederland (AHN), unmanned aerial vehicle (UAV), structure-from-motion (SfM), differential Global Positioning System (dGPS), digital terrain model (DTM), digital solid model (DSM). Note pixel resolution is that of the original data set; digital terrain models were bilinear re-sampled to 20 m.

Provider	Name	Date range	Resolution xy (m)	Resolution z (m)
UCA	In-situ dGPS	2014-2015	0.02	0.02
UCA	In-situ dGPS	2015-2016	0.02	0.02
UCA	UAV SfM DSM	2015-2016	1	0.02
UCAM	In-situ dGPS	2014-2015	0.02	0.02
UCAM	In-situ dGPS	2014-2015	0.02	0.02
UCAM	In-situ dGPS	2015-2016	0.02	0.02
UCAM	In-situ dGPS	2015-2016	0.02	0.02
DATA.GOV.UK	DTM	2009-09-26	2	0.15
DATA.GOV.UK	DTM	2015-05-31	2	0.15
NIOZ	In-situ dGPS	2014-2015	0.02	0.02
NIOZ	In-situ dGPS	2015-2016	0.02	0.02
NIOZ	In-situ dGPS	2015-2016	0.02	0.02
AHN	DTM	2015-05-31	0.5	0.01

2.5 Vegetation absence/presence

2.5.1 Educational mode

A 20 meter resolution global binary dataset indicating vegetation presence is created along the coasts of the world. This is done using Google Earth Engine. Using OpenStreetMap, a coastline raster is created along the coasts of the world. Using several bands of both Sentinel 2 and Landsat 8, cloud free imagery are selected using QA60 and QA bands for Sentinel 2 and Landsat respectively. Using the methodology of Zhu et al. (2012) a threshold indicating vegetation presence for each raster has been calculated using mean NDVI in tropical and NDVI-amplitude in temperate regions.

Corine Land Cover (CLC) map and Global Mangrove Map (Giri et al., 2011) are used to determine thresholds for vegetation *versus* no vegetation presence.



Using the described method does not deliver a single accuracy value. Accuracy of the topography input will depend on local situations and availability of imagery from both Landsat as well as Sentinel. Visual inspection of agreement of vegetation pixels with ground reference data collected at the case study sites shows a close agreement (>95% of pixels were correctly identified). This method will not detect vegetation if it is present at very low density, for instance pioneer vegetation on a bare mudflat.

2.6 Vegetation type

2.6.1 Educational mode

The global data source for vegetation type is GLOBCOVER with a resolution of 300 m. The GLOBCOVER dataset is validated using numerous points over the world as is shown in Figure 2.8.

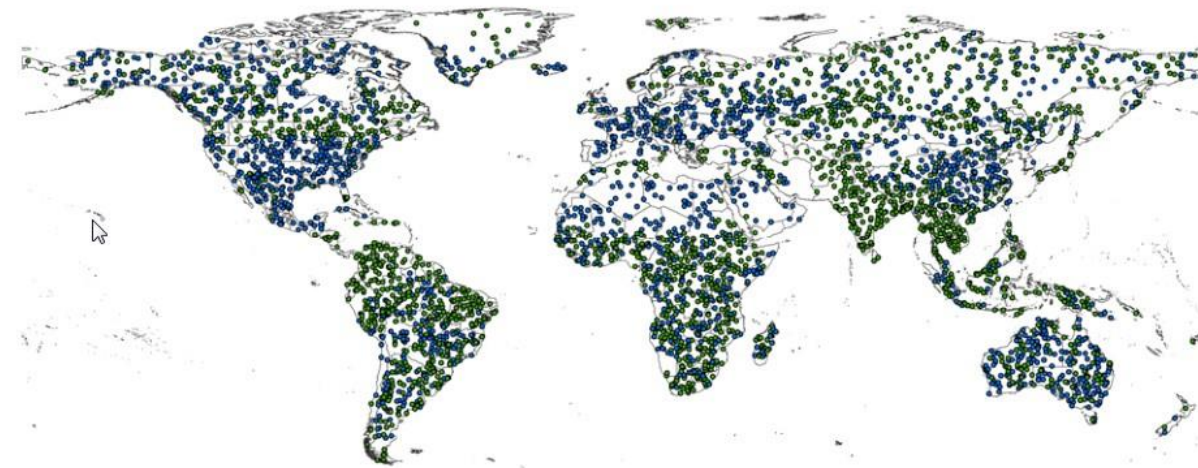


Figure 2.8 Distribution of the points sampled used for the validation of the GlobCover 2009 land cover map. Blue points are the ones derived from the 2005 database and green points are the 2009 ones (Bontemps et al 2011).

Validation is carried out visually (using all kinds of imagery ranging from Google Earth to NDVI imagery from SPOT VGT) and with expert judgment using the formerly described database (Figure 2.). MI-SAFE classifies vegetation into only a limited number of classes, these are shown in the table below, Table 2.4. It is expected that future developments may refine those classifications.

Table 2.4 MI-SAFE vegetation classes

Class number	Description
1	Intertidal vegetation
2	Intertidal flats
3	Water
4	Salt marsh
5	Broad leaved forest/Mangrove

Globcover has many classes, so these classes have been reclassified into the classes mentioned above. Table 2.5 describes this reclassification.



Table 2.5 Globcover classes (Bontemps et al 2011).

Value	Class	GlobCover global legend
11	0	Post-flooding or irrigated croplands
14	0	Rainfed croplands
20	0	Mosaic Cropland (50-70%) / Vegetation (grassland, shrubland, forest) (20-50%)
30	0	Mosaic Vegetation (grassland, shrubland, forest) (50-70%) / Cropland (20-50%)
40	5	Closed to open (>15%) broadleaved evergreen and/or semi-deciduous forest (>5m)
50	5	Closed (>40%) broadleaved deciduous forest (>5m)
60	5	Open (15-40%) broadleaved deciduous forest (>5m)
70	0	Closed (>40%) needleleaved evergreen forest (>5m)
90	0	Open (15-40%) needleleaved deciduous or evergreen forest (>5m)
100	5	Closed to open (>15%) mixed broadleaved and needleleaved forest (>5m)
110	0	Mosaic Forest/Shrubland (50-70%) / Grassland (20-50%)
120	0	Mosaic Grassland (50-70%) / Forest/Shrubland (20-50%)
130	0	Closed to open (>15%) shrubland (<5m)
140	0	Closed to open (>15%) grassland
150	0	Sparse (>15%) vegetation (woody vegetation, shrubs, grassland)
160	5	Closed (>40%) broadleaved forest regularly flooded - Fresh water
170	5	Closed (>40%) broadleaved semi-deciduous and/or evergreen forest regularly flooded - Saline water
180	4	Closed to open (>15%) vegetation (grassland, shrubland, woody vegetation) on regularly flooded or waterlogged soil - Fresh, brackish or saline water
190	0	Artificial surfaces and associated areas (urban areas >50%)
200	0	Bare areas
210	3	Water bodies
220	0	Permanent snow and ice

In this table a large proportion of vegetation is classified as Broadleaved forest/Mangroves (class 5). The MI-SAFE viewer only considers mangroves to appear between -30 and 30 degrees latitude and only on the coast, for all other instances class 5 is considered to be broad leaved forest.

For European coastlines and therefore including the study sites, the EU Corine Land Cover map (CLC2012) (<http://land.copernicus.eu>) is used. A detailed description of the classes of the CLC2012 map can be found at <http://uls.eionet.europa.eu/CLC2000/classes/index.html>. The documentation of CLC2012 states a thematic accuracy of $\geq 85\%$ and has a spatial resolution of 100 m.

This map has been reclassified into the classes described in Table 2.6 Table 2. (using the classes within the CLC).

Table 2.6 Corine Land Cover Vegetation Classes and reclassification by MI-SAFE.

grid	CLC code	CLC label	MI-SAFE label
23	311	Broad leaved forest	5 Broad leaved deciduous forest
35	411	Inland marshes	4 Inland marsh



37	421	Salt marshes	1 Vegetated intertidal
38	422	Salines	3 Water
39	423	Intertidal flats	2 intertidal flats
40	511	Water courses	3 Water
41	512	Water bodies	3 Water
42	521	Coastal lagoons	3 Water
43	522	Estuaries	3 Water
44	523	Sea and ocean	3 Water
		All remaining classes	0 No vegetation

2.7 Vegetation biophysical parameters: NDVI

2.7.1 Expert mode

In EU FAST, Sentinel-2 data are atmospherically corrected using Sen2Cor in SNAP to obtain surface reflectance images, and the NDVI is calculated based on surface reflectance in band 4 (red) and band 8 (near-infrared) in each image, while the Leaf Area Index (LAI) of the marsh is retrieved from the level 2 biophysical product after Sen2Cor atmospheric correction, provided $NDVI > 0.3$ (marsh only).

In this validation exercise as performed by NIOZ, we will address the uncertainties associated with (1) atmospheric effects in assessing the NDVI and the LAI and (2) the relationship between in situ and satellite NDVI.

For the validation, Sen2Cor corrected imagery of the Zuidgors site in the Netherlands were considered for overpasses during cloud-free low tide conditions in 2016, matching large field campaigns in January 2016 and May 2016. Empirical lines were established with surface reflectance values extracted at semi-invariant pixels (roof tops, asphalt, deep clear water etc.) in the images, with a clear, low tide Sen2Cor corrected image of 12 March 2016 used as a reference. The empirical lines had excellent linear fits (typically $R^2 > 0.95$), but with some differences in offset and gain (Figure 2.9).

The empirical line calibrations (ELC) were then applied to bands 4 and 8 of the 25 January 2016 and 1 May 2016 image after Sen2Cor atmospheric correction, and used to calculate an ELC corrected NDVI. The Sentinel-2 NDVI with Sen2Cor correction and the Sentinel-2 NDVI with Sen2Cor and ELC correction were then compared to the NDVI measured in situ with a TRIOS Ramses spectroradiometer (with in situ spectra resampled to the band settings of Sentinel-2, taking into account the spectral sensitivity of Sentinel-2). In situ measurements were carried out on 1 m² plots on the foreshore and in the saltmarsh, where each plot was represented by an average of 5 in situ measurements (see field protocol reports). The in situ measurements were performed on 19 and 21 January 2016 (large campaign January 2016), and on 19 May 2016 (large campaign May 2016), also by NIOZ.



The regression lines of in situ versus satellite images fit well (Figure 2.10), although within the cluster of saltmarsh vegetation (i.e., high NDVI) and within the cluster of bare sediment (i.e., low NDVI), the fit is moderate only.

The in situ and satellite data from January 2016 approach the 1:1 relationship. However, the satellite NDVI of 1 May 2016 is lower than the in situ NDVI of 19 May 2016. The effect of the ELC is minimal. Hence, it can be concluded that the Sen2Cor atmospheric correction, as applied in the EU FAST products of NDVI, is adequate. Possible explanations for the deviation from the 1:1 line for the May 2016 data may likely include a mismatch in time (that is, in situ data represent a situation later in the growing season, with possibly higher NDVI than the NDVI in the S2 satellite image of a few weeks earlier, see for example Figure 3.1 for development of LAI in time), and possibly differences in conditions during acquisition and/or NDVI saturation effects.

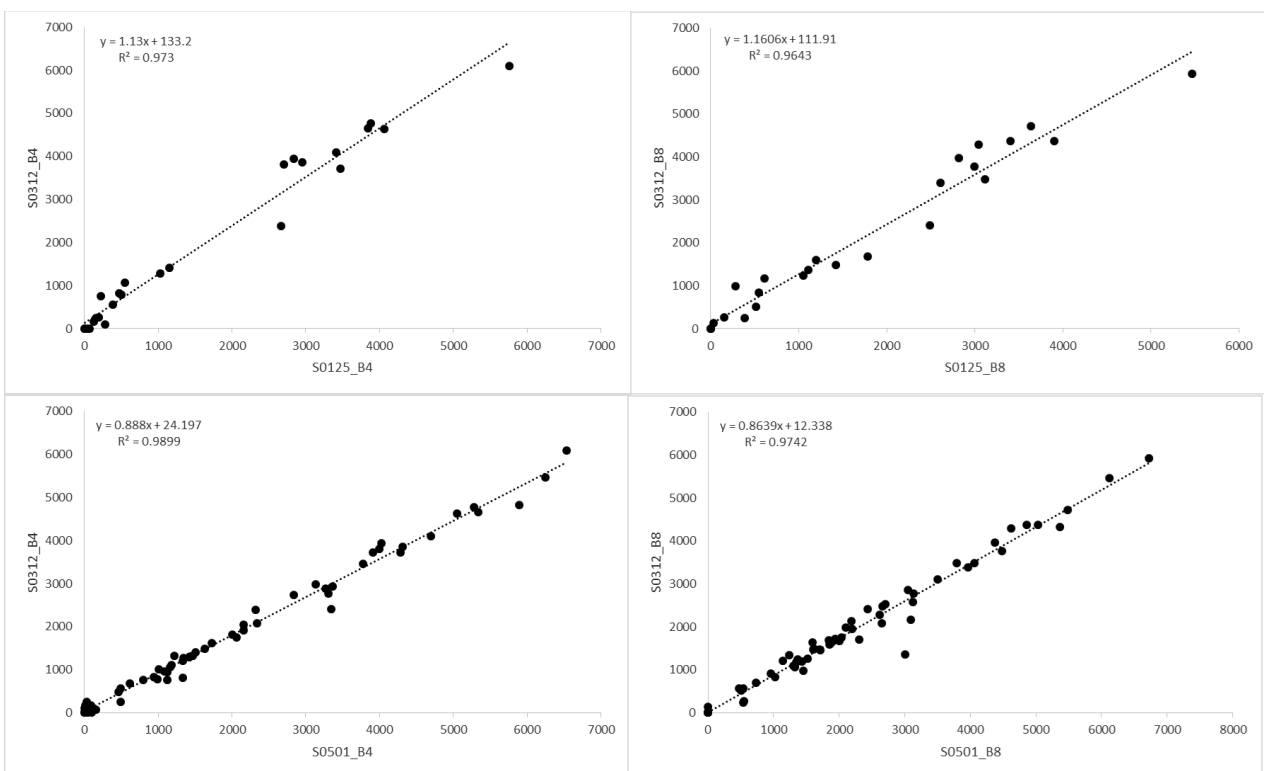


Figure 2.9. Validation of atmospheric effects by an Empirical Line Calibration (ELC). Comparison of surface reflectance after Sen2Cor atmospheric correction in semi-invariant pixels in Sentinel-2 bands 4 and 8 in the reference image (12 March 2016, y-axis) and target images (25 January 2016 for row above, 1 May 2016 for row below, x-axis).



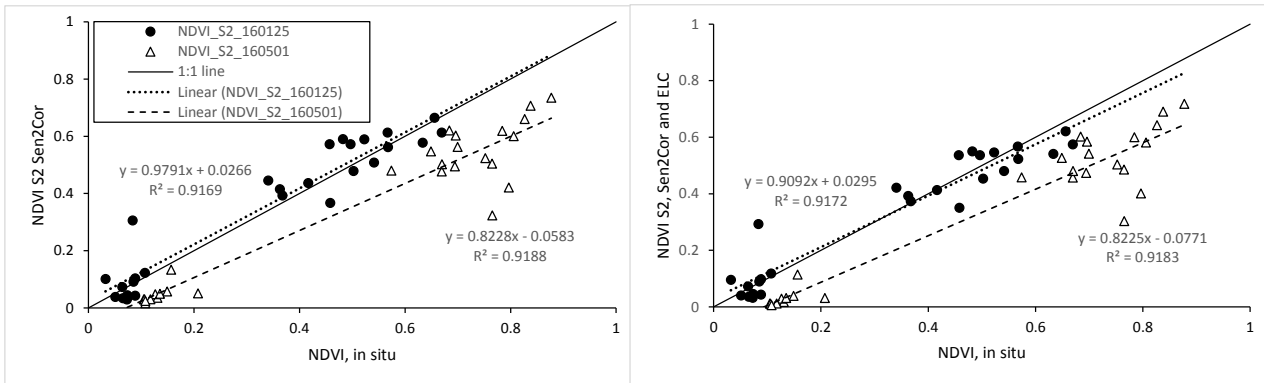


Figure 2.10. Validation of the NDVI, Zuidgors, the Netherlands. Average NDVI measured in situ at field plots (x-axis) versus NDVI from Sentinel-2 after atmospheric correction with Sen2Cor (left) and after correction with Sen2Cor and an ELC (right), as defined in the previous figure. Black dots show in situ NDVI from 19 and 21 January 2016 versus NDVI based on a Sentinel-2 image of 25 January 2016. White triangles show in situ NDVI from 19 May 2016 versus NDVI based on a Sentinel-2 image of 1 May 2016. The dotted lines show a trend line based on linear regression. The solid line is the 1:1 line.



3 Output

3.1 Model description

In order to quantify wave attenuation by vegetation for a given salt marsh or mangrove coastline, the MI-SAFE viewer uses the numerical modeling software XBeach-VEG (van Rooijen et al., 2016). XBeach is a depth-averaged, two-dimensional process-based model that solves the time dependent short wave action balance for the entire wave group, suitable for simulating wave attenuation over foreshores. XBeach has three wave energy dissipation processes relevant for MI-SAFE simulations: dissipation due to (depth-induced) wave breaking, dissipation due to bottom friction and dissipation due to vegetation. XBeach also has three simulation modes, from simple to advanced: stationary, surfbeat and non-hydrostatic. The stationary mode is fast but lacks wave groups (surfbeat) that are important for wave height variations near the shore. The non-hydrostatic mode is physically the most complete but at substantial computational cost. The surfbeat mode does represent the effects of wave groups at reasonable computational cost and represents the effects of vegetation via the well-known relations of Mendez & Losada (2004), and is therefore selected as the most useful mode for this application.

3.1.1 Educational

For the Educational version, XBeach was used to generate a lookup table of attenuated wave heights for a range of possibly occurring combinations of nearshore waves and water levels, foreshore slopes and -widths and vegetation types. The MI-SAFE viewer searches this table using the conditions at the selected site as input, resulting in a reduced wave height at the end of the vegetation where any coastal protection is structure or higher ground is located. Subsequently, this reduced wave height is used to calculate a reduction in required crest height (based on the EuroTop relations from Pullen et al., 2007) of a standard embankment-type protection structure with grass cover on 1:3 sloped embankment, in comparison with a bare foreshore under the same forcing. This standard embankment type is chosen to facilitate comparisons between locations and to illustrate what wave height reduction means for the dimensions (i.e. cost) of a flood defense; required crest heights for other embankment types can be calculated using the wave height at the end of the vegetation and appropriate parameter settings in the EuroTop relations.

3.1.2 Expert

For the Expert version of the MI-SAFE viewer, a number (typically 6) of ~ 2 km long transects has been defined at each study site, running from the near shore to the position of the coastal protection structure estimated from EO images. At some sites (NL, UK) the foot of the protection structure can be clearly distinguished, on other FAST field sites (RO, ES) the relevant end of a transect is more difficult to define. For all transects, dedicated site-specific XBeach simulations have been performed using the local bed level, hydraulic boundary conditions and vegetation cover. Just like in the Educational version, this results in the attenuated wave height at the foot of the protection structure. This is then used to calculate the required crest height. It does so, however, with much greater precision because the actual situation is simulated rather than results being selected from a previously simulated model run that provides a close, but not exact, fit to the



selected location. For three storm surge events (return periods: 1/10 (10%), 1/100 (1%) and 1/1000yr (0.1% likelihoods), the model has been run for each transect.

3.1.3 Advanced

For one study site (Tillingham, UK) the model has been applied in an advanced modality. In this case a complete 3D non-hydrostatic calculation was realized, resulting in wave attenuation over a half tidal cycle assuming a 1/100year (or 1% likelihood in any one year) storm surge event.

3.2 Calibration of output

To ensure that model calculations provided reliable outputs for all possible relevant situations, the XBeach model was calibrated by adjusting model parameters and forcing it within the margins of the uncertainties. A hydro- and morphodynamic calibration was conducted for a vast range of lab and field cases. For vegetation, the model was calibrated based on wave observations data in combination with the Leaf Area Index (LAI) from the Earth Observation data.

3.2.1 Hydrodynamics without vegetation

The XBeach code and related functionalities are undergoing continuous development. As a result there is a need from modellers and code developers to develop a tool that provides insights into the effect of code developments on model performance. The XBeach skillbed (URL: <http://oss.deltares.nl/web/xbeach/skillbed>) tries to fulfil this need by running a range of tests, including analytical solutions, laboratory tests and practical field cases every week with the latest code.

Based on this document one can conclude that for the lab and field cases in the skillbed, XBeach is capable of resolving short and long wave propagation, sediment transport and morphological development without vegetation. For a more elaborate analysis of the model calibration, refer to Roelvink et al. (2009).

3.2.2 Wave attenuation due to vegetation

When modelling vegetation in XBeach, the model requires four parameters to represent the presence of vegetation:

- 1) length or height h (m);
- 2) width or diameter d (m);
- 3) number of stems per horizontal area n (m^{-2});
- 4) drag coefficient C_D (-).

The product of all parameters is the vegetation factor, which can be regarded as an 'effective biovolume' related to wave attenuation. The product of n , d and h is the Leaf Area Index (LAI), which can be derived from EO. For deriving representative properties based on biophysical characteristics under 'Data', three principles were followed:

- 1) The vegetation factor should be relatively conservative, so as not to give an overly optimistic estimate of wave attenuation. Thus, plant dimensions are chosen with winter conditions and relatively small individuals in mind. The choice of the drag coefficient *a priori* is troublesome, because this coefficient not only depends on the plant properties above but



also on the hydrodynamic conditions. Therefore, a relatively conservative estimate is made with large waves (that give large Reynolds/Keulegan-Carpenter numbers that are associated with low drag coefficient values) and the flexibility of the vegetation in mind. This can be refined once more reliable drag coefficient estimators are available, e.g. based on observations under (near-) design conditions in large-scale flume experiments. The flume work done by Möller et al. (2014) is an important basis for the estimation of the drag coefficient as it is representative for near design conditions (for UK coast).

- 2) The vegetation factor should be representative for all occurrences of a particular vegetation type, not just for a specific site.
- 3) The vegetation factor should be large enough and differ enough between vegetation types to meaningfully differentiate the effects of different vegetation covers from each other.

3.2.2.1 Vegetation types

The table below (Table 3.1) shows how the different vegetation types are characterised in terms of XBeach input parameters. Note that these basic assumptions are used if only global information is available in the Educational version of the viewer at present. In the Expert version, the local EO data are used to derive vegetation properties.

- For salt marshes, the values were defined based on the field observations at the FAST field sites, the properties of the temperate marsh tested by Möller et al. (2014) and the global inventory of Songy (2016). The drag coefficient of 0.19 is the lower limit found in the large flume tests by Möller et al. (2014); Songy (2016) matched field observations by Vuik et al. (2016) using a drag coefficient of 0.4. These values are well below the textbook value of ~ 1 for stationary flow through cylinders due to the flexibility of the vegetation. *Spartina*, *Elymus* en *Puccinellia* species are the dominant species that are represented in the experiments.
- The mangrove parameters are based on the inventory of Janssen (2016), who synthesized observations of a.o. Cole et al. (1999), Narayan (2009), Mazda et al. (2006) and Horstman et al. (2012). Here, the representative drag coefficient could not be derived from experimental results since high quality observations on wave attenuation by mangroves under storm conditions do not exist. Instead, the theoretical value for a circular cylinder was used as mangrove trunks can be considered to be rigid.
- Reed beds are fully parameterized based on the observations at the Romanian field sites, the drag coefficient is chosen lower than 1 but higher than the 0.19 used for salt marshes to account for the greater rigidity of reeds.
- The properties of willows have been measured in two projects of Deltares (unpublished) along rivers in the Netherlands. For this vegetation type, the drag coefficient is chosen equal to that of mangroves, for the same reason of missing observations.

The calculated wave attenuation is very sensitive to the value of C_D . While the FAST dataset includes a much wider range of vegetation types for which coefficients are empirically determined, further flume and/or field experiments that provide better estimations of this coefficient for vegetation types not present at FAST case study sites, would greatly enhance the quality of simulations and thereby the applicability of nature based flood defences.



Table 3.1 Vegetation input parameters to XBeach model. n = number of stems per m^2 , d = diameter of the stems, h = height of the stems, C_D = drag coefficient.

Type	n (m^{-2})	d (mm)	h (m)	C_D (-)	nd (m-1)	vegetation factor (-)
salt marsh	1225	1.25	0.30	0.19	1.53	0.087
Reeds	77	10	2.6	0.60	0.77	1.2
Broadleaved forest: mangroves	30	35	3.0	1.0	1.05	3.2
Broadleaved forest: willows	15	8.4	3.4	1.0	0.13	0.43

Note that salt marsh vegetation is the shortest vegetation, which means that, while it is effective in reducing wave height/energy, it is most effective at low inundation depths. The taller reeds, mangrove and willows with their taller and stiffer structure are relatively more effective at larger inundation depths.

Changes in vegetation cover over time and also the spatial heterogeneity of the vegetation cover will affect the wave attenuating capacities of the foreshore. For engineering evaluations of coastal protection structure safety, it is important to know this variability in order to establish a safe – but not overly conservative - method for the estimation of the drag induced by the vegetation cover: a lush foreshore in summer will attenuate waves more than the sparse winter vegetation. And because coastal protection structure safety evaluations are typically performed over representative stretches of structures of several hundreds of meters long, one needs to make sure that the possible long-shore variability in vegetation cover is represented in the schematization of the cross-shore transect that is assessed.

3.2.2.2 Seasonal and spatial LAI variation at Zuidgors (NL)

The seasonal variation in vegetation cover (LAI) at the Zuidgors (NL) site is considerable, as Figure 3.1 shows. In March 2016, the average LAI over a transect along the marsh (Figure 3.2) was 0.50 (practically equal to the field-based LAI of the preceding December-January as reported in D5.4), increasing to 0.79 in April and growing further to 3.34 in mid-July of the same year. The (trend in) these along-marsh values are very similar to (the trend in) the cross-marsh values shown in Table 3.2, which indicates that the heterogeneity of the vegetation cover is isotropic.

In the same period, the spatial heterogeneity also increases as seen in Figure 3.1 and Figure 3.2: In March, LAI is either absent or very uniform around 0.5 all along the marsh. One month later, LAI has increased to around 1 on the eastern part of the marsh but remains around 0.5 at the western end. In this month, the LAI starts to display areas with lower vegetation cover, which is most clear between 1200 and 1400 m. In May, the same pattern is visible for a higher overall LAI (1-1.5) but now the bare areas between 400 and 800 m have been vegetated; vegetation density in the west and between 1200-1400 m remains lower. The situation in July is very similar to that in May, for a substantially higher LAI of around 4 on the well-vegetated parts of the marsh; the lower LAI in the West and between 1200-1400 m remains well visible. Using the standard deviation of the LAI as a



proxy for the spatial variability quantifies these visual observations: The standard deviation of the LAI along the longitudinal transect goes from 0.10 in March via 0.23 in May to 0.92 in July.

A technical note: Because XBeach requires a vegetation type file for every different plant density, the number of input files can become excessively large for computations with large areas of heterogeneous vegetation. To avoid this, vegetation with similar N has been grouped into a limited number of classes. For the configuration at Zuidgors, it was found that ten classes provide enough detail to give less than 1% error in the estimation of the wave height at the foot of the sea defence structure.

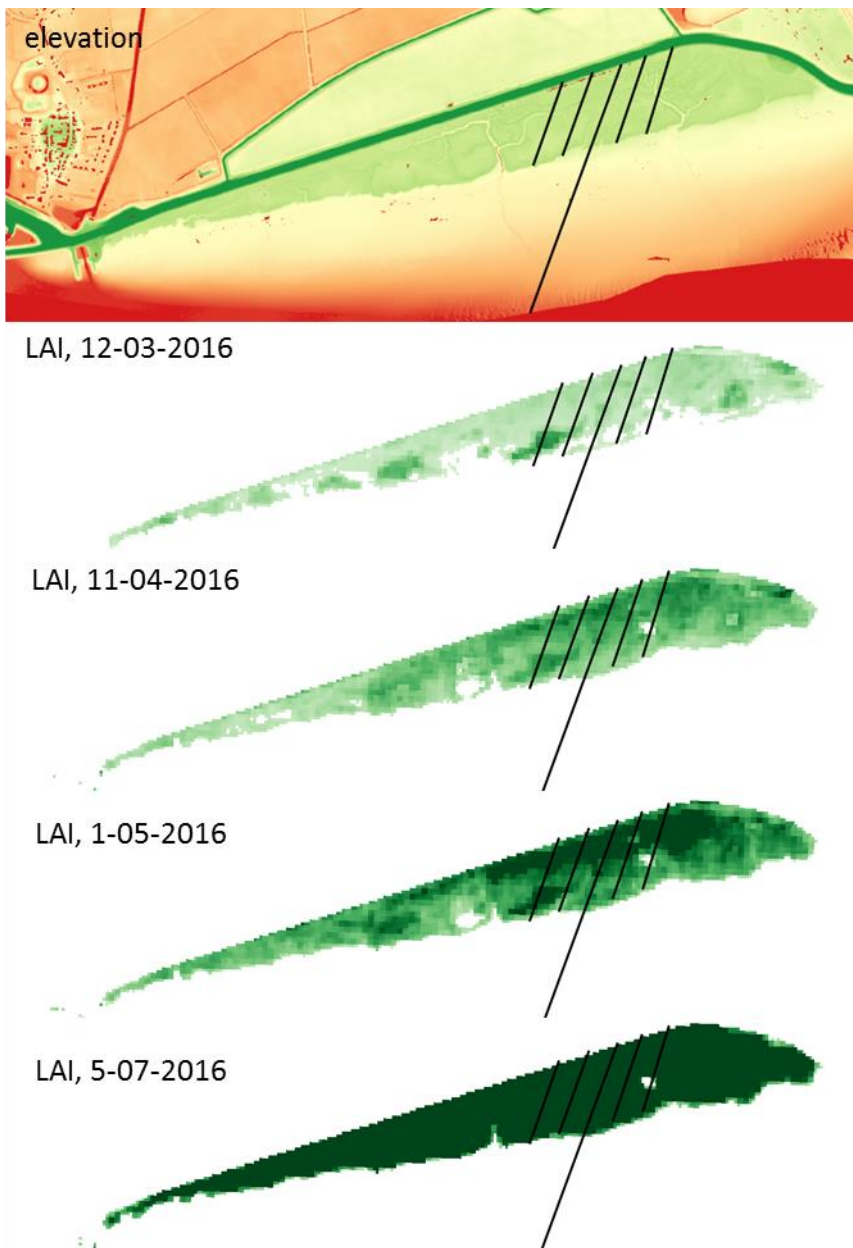


Figure 3.1 Elevation (from AHN, table 2.,2) and seasonal changes in Leaf Area Index of the Zuidgors (NL) fieldsite; darker colours indicate higher LAI. The long transect is the one used to assess seasonal variation and effects of LAI under/overestimation, the shorter transects are used to evaluate spatial variation.



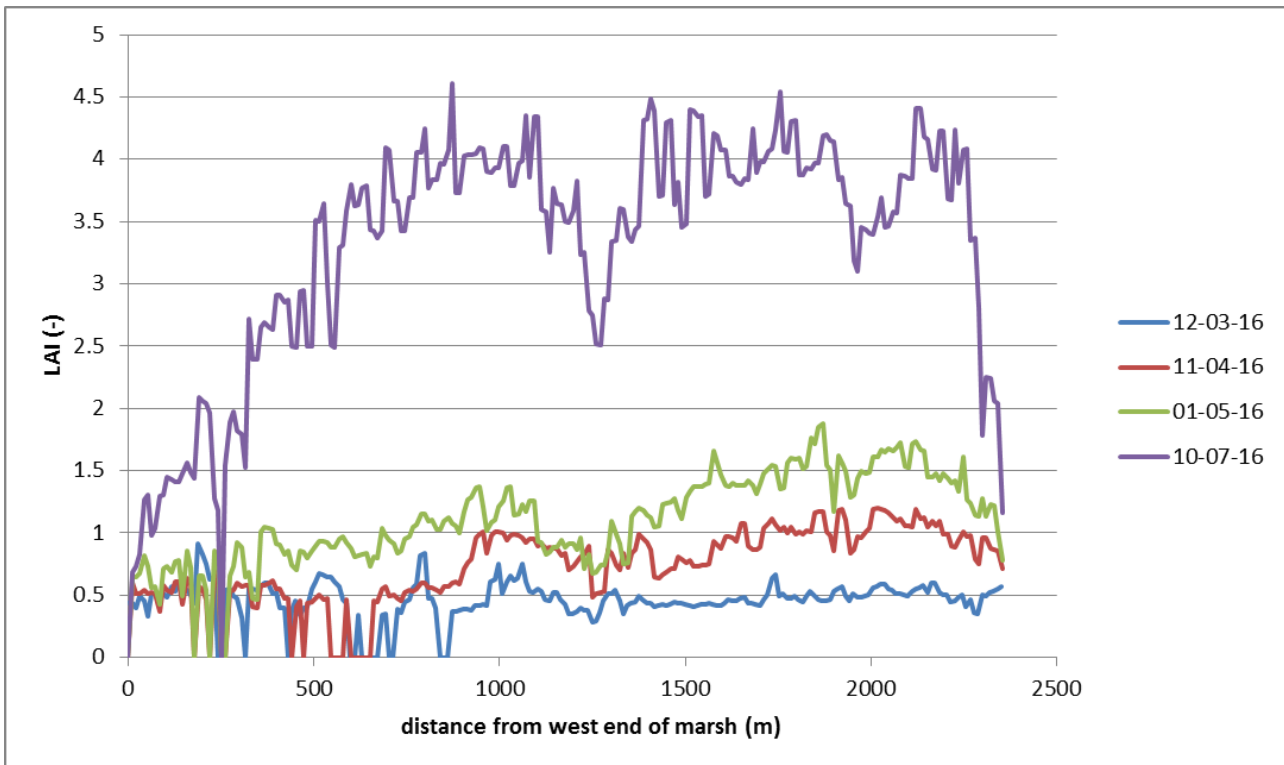


Figure 3.2 Variation in LAI along the shore of the Zuidgors (NL) salt marsh, for the same dates as Figure 3.1.

3.2.2.3 Effect of seasonal LAI variation on wave properties

To quantify the effect of seasonal variations in LAI on engineering variables, the four temporal LAI covers are placed on the same, slightly simplified cross-shore transect (see Figure 3.3, the location of the transect is indicated by the long line in Figure 3.1) to compute the wave attenuation using XBeach and the required crest height using the Eurotop formulae (Pullen, et al., 2007; see D5.4). The detailed bed level (0.5 m horizontal resolution) was taken from the LiDAR-generated Detailed Elevation Model (DEM) 'Actueel Hoogtebestand Nederland' (AHN). The transect was simplified to evaluate purely the effect of different vegetation covers by ruling out effects of bed topography, and extended in a seaward direction to facilitate a correct incoming wave boundary condition. For the boundary conditions, the 1/100 (1% likelihood) year return conditions for this location were used: offshore wave height $H_{rms}=7.11$ m, peak period $T_p=12.7$ s and water level (tide + surge) 4.55 m above MSL.

The different degrees of seasonal vegetation cover lead to substantial (>50%) differences in significant wave height ($H_{s,levee}$) and required crest height (RCH) at the landward limit of the cross-shore transect, see Figure 3.4 and Table 3.2. Logically, the largest wave attenuation occurs at the time of year with the highest vegetation cover, in July. From this, it can be concluded that it is unsafe to use the summer conditions of a marsh when assessing coastal protection infrastructure safety: the overestimation of wave attenuation would be large if a storm occurs in winter. On the other hand, using actual EO-based winter LAI rather than the 'standard marsh'¹ LAI conservatively

¹ The 'standard marsh' parameter values are used in MI-SAFE to allow Xbeach to calculate a result if no LAI is available. Standard marsh LAI value is derived from on the ground field measurements in FAST study sites (using $LAI=N \times l \times d$).



defined in D5.4 can give a substantial reduction in required crest height, thus construction costs, for a marsh width of 300 m.

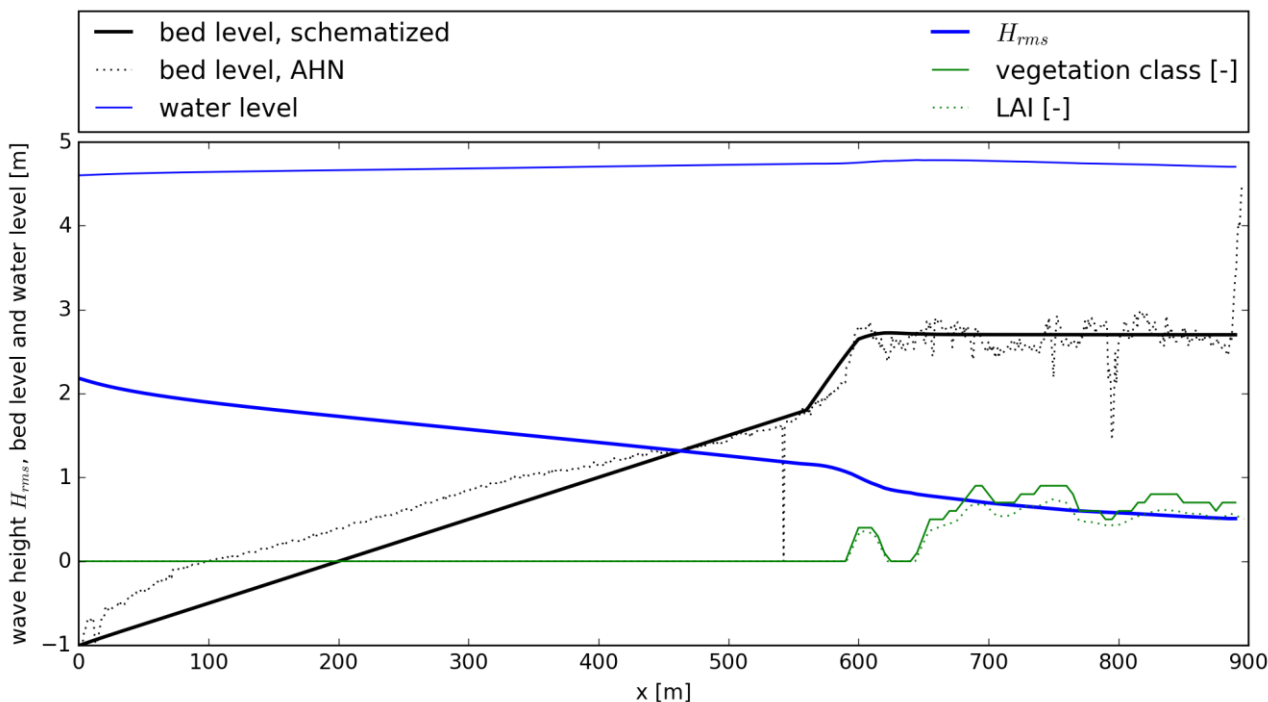


Figure 3.3 Schematisation of the long (default) transect in XBeach. The vegetation classes (continuous green line) follow the changes in actual LAI (dotted green line) well.

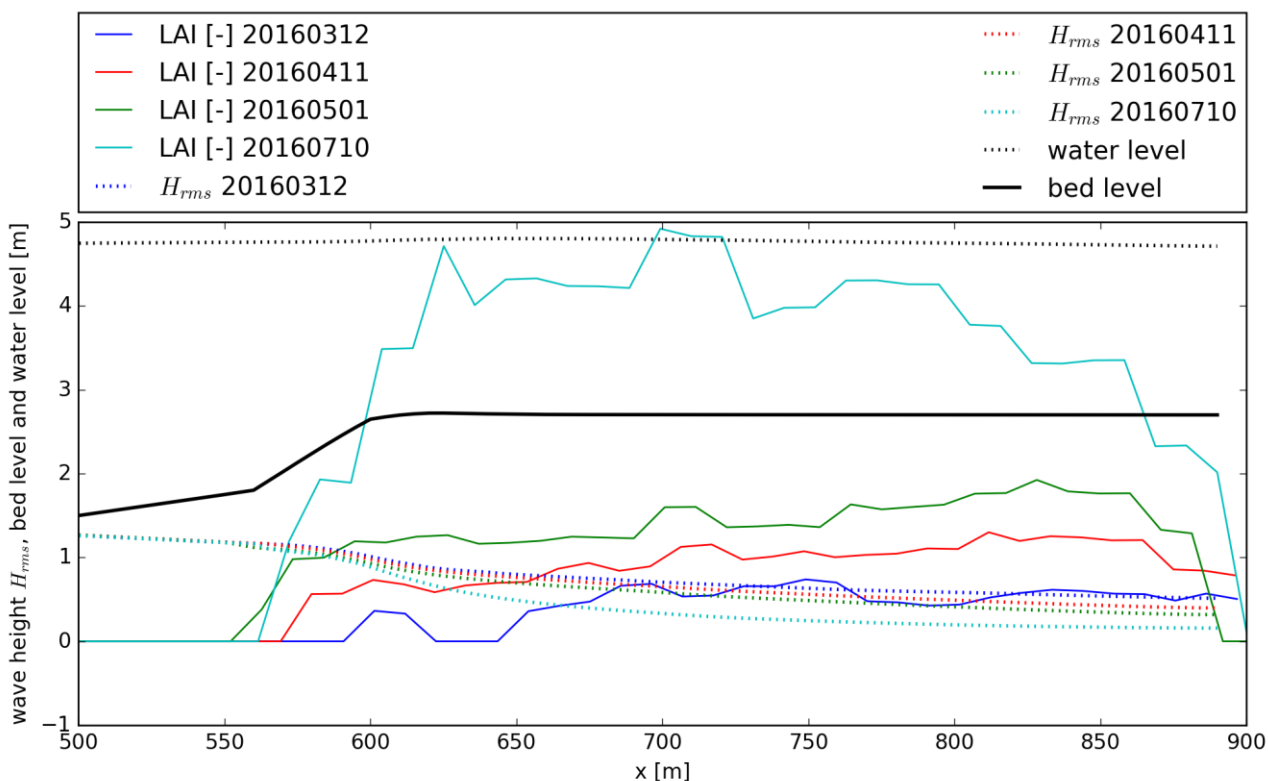


Figure 3.4 Seasonal variation of LAI and the effect on wave attenuation over the default transect at Zuidgors. First part of the transect is not shown in this plot.



These variations in vegetation at Zuidgors were used to analyse the sensitivity of the wave height at the toe of the sea defence structure and the sensitivity of the required crest height to the seasonal variation in XBeach output (Table 3.2).

Table 3.2 Indication of the seasonal variation in LAI at Zuidgors (across marsh mean and standard deviation over for default transect) and the effect on wave height at the toe of the sea defence structure as well as on the required crest height (RCH). Conservative estimate of LAI values (for instance 1SD) leads to higher RCH. Note that Sentinel 2 LAI observations are designed to deliver better than 10% error.

Date	LAI, mean	LAI, 1SD, %mean	H _{s, @levee} [m] Mean	RCH [m], Mean, +1SD, +S2:10%
2016-03-12	0.54	0.11, 20%	0.72	1.89, 2.28, 2,50
2016-04-11	0.94	0.22, 23%	0.56	1.46, 1.80, 1,98
2016-05-01	1.39	0.31, 24%	0.45	1.16, 1.42, 1,56
2016-07-10	3.65	0.95, 26%	0.22	0.52, 0.66, 0,72
Standard marsh (field observations)	0.24	0	0.84	2.25
Bare foreshore	0	0	0.96	2.66

3.3 Model inaccuracies

Process-based models, like XBeach, are not perfect. For example, in a random sequence of waves individual waves do not (all) follow the prescribed wave breaking formula. Moreover, in reality the landscape does not consist of grid cells and a homogeneous "vegetation type". To account for processes that are not explicitly modelled black-box terms like the vegetation drag force (C_D) or the bed roughness are used. Calibration and validation of models is therefore vital. But after critical inspection of what a model can and cannot do (i.e. comparison of model outputs against observed measurements), it is possible to test hypotheses and assess, for example, the relative importance of vegetation on wave overtopping. When a model uses the correct boundary conditions and proper calibration is carried out, errors tend to be small (scatter index of 6%, see van Rooijen et al., 2016).

3.3.1 Educational mode

The Educational version of MI-SAFE uses a library of 32760 (d.d. April 2017) pre-computed XBeach simulations to provide the user with results. The conditions used to construct the library are chosen to cover the range of all possible conditions (i.e. parameter space, see Songy, 2016 for the analysis), but contains, by definition, a limited number of parameters and parameter values (Table 3.3).

The pre-computed values are stored in a lookup table for wave attenuation. This introduces errors when the area of interest cannot be exactly matched with the modelled parameters (e.g. wave height of 1.75 meter is not pre-computed and an average value between 1.5 and 2 meter is used).



In addition, there are parameters which are not taken into account at all (for instance realistic bathymetry transects versus the schematized modelled transect that uses a straight line with a best fitting slope as an approximation, Figure 3.5).

Table 3.3 Uncertainty of individual parameters can be quantified (e.g. SRTM has a 9 meter vertical resolution; see Section 2), however how input uncertainty relates to model (in)accuracy has not explicitly been analysed within the FAST project. One of the largest sources of model uncertainty are the inaccuracies of global data sets representing local situations (e.g. realistic bathymetry or boundary conditions). It is possible to take into account input uncertainty in a Bayesian probabilistic network. Table 3.3 Parameter space of the educational version

Parameter	Range
Wave height (Hm0) [m]	1, 1.5, 2, 2.5, 3, 3.5, 4, 4.5, 5, 6, 7, 10
Wave steepness (s) [-]	7, 15, 30
Water level (zs) [m+MSL]	1, 1.5, 2, 2.5, 3, 3.5, 4, 4.5, 5, 6, 7, 8, 10
Vegetation type [-]	0: no vegetation 1: salt marsh 2: mangrove 3: large reeds 4: willows
Coastal slope [-]	10, 20, 40, 70, 100, 150, 200, 250, 300, 400, 600, 800, 1000, 2000

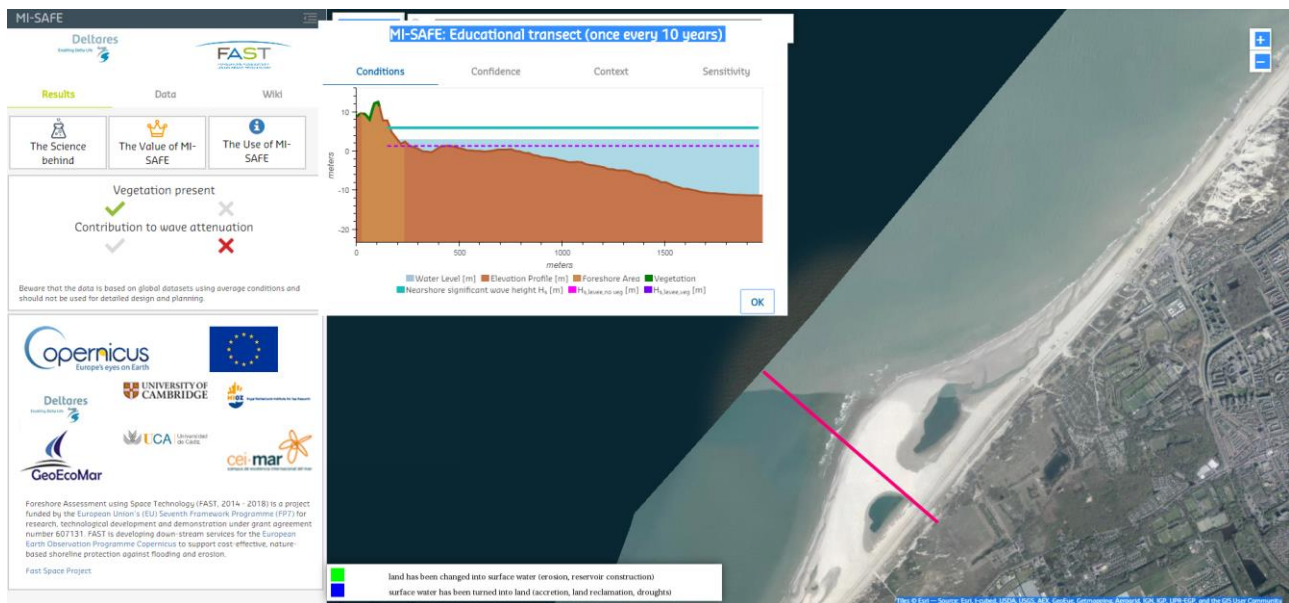


Figure 3.5 An example transect of the educational version showing the difference between the satellite image and the determined transects at the Sand Motor, the Netherlands.

To give some sense of possible error, the difference in wave attenuation (consequently, required crest height) has been assessed for a set of deviations around a ‘common’ condition: A 250 m wide salt marsh with a slope of 1:250 m, offshore significant wave height of 2.5 m and a water level of 4.5 m above MSL. Since in the Educational version the slope is usually the most uncertain parameter because the global elevation datasets GEBCO and SRTM come with large uncertainties,



the slope is varied with around 25% around this value and around both a considerably steeper (1:70) and considerably flatter (1:800) slope. The exact magnitude of variations depends on the nearest values in the lookup table, which means that the differences not only reflect a possible error due to inaccurate slope estimations but also due to the discrete number of slopes in the table. For steep slopes, the effect (difference between ‘correct’ and steeper or flatter in Table 3.4) is larger (close to 30% under or over estimation of wave attenuation) but levels off as slopes become flatter (2-3% error in wave attenuation). In that regime, the presence of vegetation –and the errors in vegetation related parameters- become more important as can be derived from the increasing difference between the columns ‘veg’ and ‘no veg’ (just 1-2% at steep slopes going to 7-8% for flat slopes).

Table 3.4 Percentage wave attenuation $[100 \cdot (H_{\text{levee}} - H_{\text{nearshore}}) / H_{\text{nearshore}}]$ over a foreshore width of 250 m for a +/- 25% error in slope estimates, for steep, common and flat foreshore slopes. At very steep slopes, waves are fully attenuated.

	Steep (1:70)		Common (1:250)		Flat (1:800)	
	Veg	No veg	Veg	No veg	Veg	No veg
Steeper	100	100	37	30	31	23
‘Correct’	71	70	36	30	29	21
Flatter	51	49	34	27	28	21

3.3.2 Expert mode

The advantage of the expert mode is that data with the highest accuracy available is used to create and drive dedicated XBeach models. Model inaccuracies related to the limited parameters space and global data sets are therefore not present anymore. Especially a big improvement is related to the more accurate bathymetry and topography data that can be used in the expert version. However, there are still model inaccuracies present due to data and model formulations (see also 3.3).

Even the most accurate data still contains errors. These errors can either be related to date of the data (e.g. bathymetry was measured five years ago) or the source. The latter is the case when using state-of-the-art EO-derived maps about the presence of vegetation (see Section 2.7) in which there are inaccuracies in the analysis technique. Presumably, the error related to the global boundary conditions for water levels and waves and the specification of the vegetation properties are dominant in the expert version.

3.4 Challenges

3.4.1 Educational modality

The use of global data, which was not derived with the specific objective of the MI-SAFE viewer in mind, provides a number of challenges related to the resolution of the data and assumptions made to be able to combine this data. After extensive testing, the viewer provides results in many areas, but quality issues remain. In general, we are driving the model with storm surge and wave data



from the best available global dataset, but for any specific location this is less precise input than could be wished for. Furthermore, for coastal bathymetry and elevation we are using datasets that are known to be inaccurate on a decameter scale (The vertical accuracy of GEBCO is unknown and SRTM is +/- 9 meter –but seems more accurate at many locations; see more in Section 2). In our case we improved this map by adding a specially produced intertidal map, improving the elevation information in horizontal and vertical resolution in a crucial part of the foreshore (GEE-IE). However, if there is no tide in the area, or shores are very steep, this map is not available and we fall back to using the lowest quality maps available in the viewer.

In specific situations that are difficult to capture with global algorithms the quality of results is most uncertain:

1. The MI-SAFE viewer uses a number of ‘standard’ vegetation types (salt marsh, reeds, mangroves) with standard dimensions because identifying the exact species composition from present EO data is not possible. This introduces two types of uncertainties: the vegetation type derived from e.g. Globcover may not be representative for what is actually on the ground, and the actual characteristics of the vegetation are not taken into account in the educational modality.
2. The transformation from offshore waves to nearshore waves in the Educational modality is simply depth-limited because a statistically and physically correct derivation of locally representative wave conditions requires too much computational effort (multiple minutes till several hours) within the viewer while interacting with the user. This simple algorithm works well on most open, exposed locations but fails where the area of interest lies within a sheltered bay, lagoon or estuary environment where waves are predominantly generated by local winds or where diffraction becomes important.
3. Around shallow foreshores, the bathymetry and the position of the coastline may change considerably within a few years, especially near river mouths with substantial sediment supply or rapidly retreating coasts. The global bathymetry, SRTM and coastline vector maps do not reflect most recent changes. The maps produced in FAST is using the latest imagery or local datasets where possible. However, it is a challenge keeping the information updated beyond the lifetime of the project itself.
4. The continuous bathymetry-elevation map of a transect is stitched together for 3 parts (GEBCO, GEE-IE and SRTM). At the stitching-locations, cross-shore profiles may show strange height transitions. The transition from GEE-IE to SRTM can show high ground where the SRTM begins, but this can be due to SRTM including tree top height as ground level. Especially at coasts where forests are bordering the sea. Without local information, it is not possible to correct for such errors (see figure 3.6).
5. There is no global database on location or properties of flood defences (levees), which necessitates the assumptions that 1) such a structure is present at the location where the vegetation on the foreshore ends and 2) all such structures have the same basic layout. With more information on coastal defence structures, the assessment of flood risk reduction can be more meaningful.
6. Model outputs are driven by data on waves, storm surge levels and bathymetry. In the educational modality the approximation by using a pre-computed library and transformation of offshore to nearshore waves is causing limited quality of outputs. The greatest challenge



is to increase this quality by further increasing the quality of the inputs for all relevant coastlines of the world.

7. The model output and the relative importance of vegetation information is related to combinations of model inputs for each location. This was shown in Table 3.4. Model inputs are not precise because of uncertainties in input data quality. How the combined uncertainties of all the individual inputs precisely relate to uncertainties in the prediction of the model is not made explicit within the online Educational and Expert modalities of FAST. However, the qualities of the inputs are made explicit in the viewer (the 'Confidence' tab in the results pop-up window). A challenge is to establish this detailed relation between input and outputs. This can be achieved, for instance, by feeding a synthetic database of representative bathymetric and hydrodynamic properties in a Bayesian probabilistic network. This is an advanced service that can be provided to specific uses for specific cases.

3.4.2 Expert modality

For the Expert modality of the MI-SAFE viewer, which uses local and therefore more accurate information in combination with dedicated XBeach calculations, some challenges still remain:

1. Retrieval of Leaf Area Index from EO data has uncertainties. In the Sentinel-2 mission requirement document, a goal accuracy of LAI is given of 10%. Recent projects (e.g., ESA VALSE2) address the validation of Sentinel-2 biophysical products with field data. In EU FAST, Leaf Area Index was not directly measured in the field, and hence, the field measurements could not be applied to establish accuracies of the retrieval of satellite Leaf Area Index. The field data of biophysical vegetation measurements collected in EU FAST (stem density, stem height, vegetation biomass, etc) will be used to evaluate the relationship with satellite derived biophysical measures.
2. Drag coefficients for vegetation under extreme hydraulic loads are still surrounded with large uncertainties that can only be resolved by real-scale wave flume experiments. The filed measurements executed in FAST did not capture these extreme conditions.



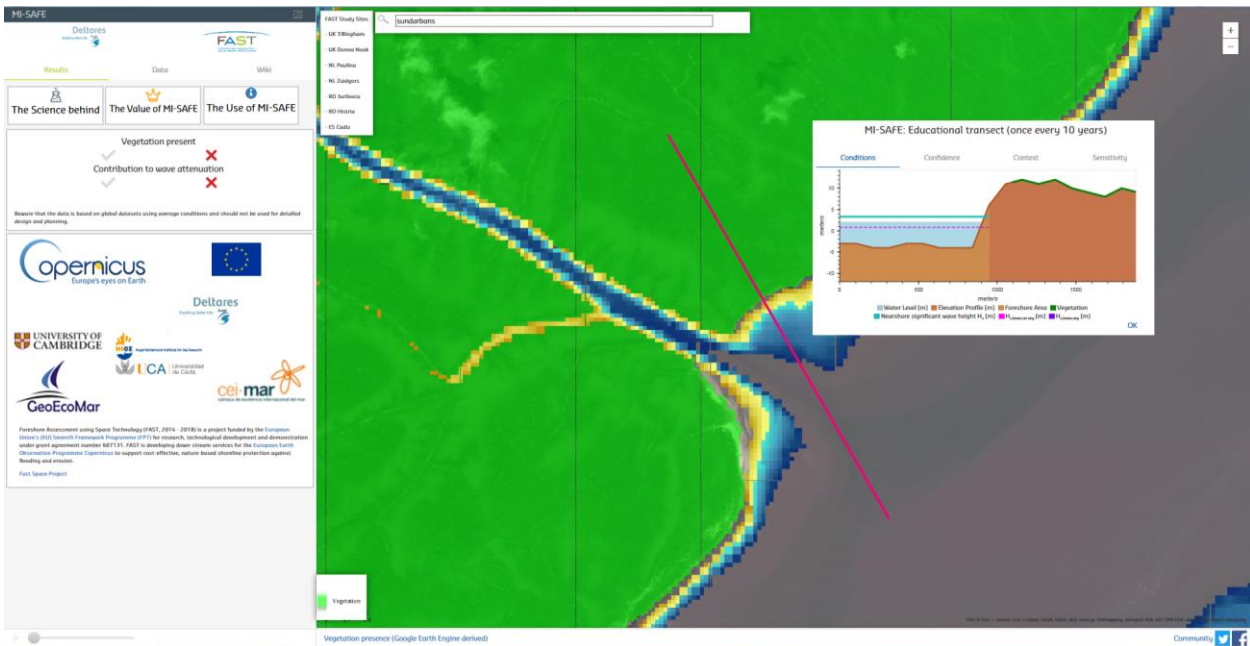


Figure 3.6 An example transects of the educational version showing the transition between GEE-IE bathymetry (light brown in graph) and SRTM elevation (dark brown in graph) somewhere in the Sundarbans (Bangladesh). It is possible that SRTM includes the tree height as ground level. (green colours in map show vegetation presence, brown-yellow-blue hues show GEE-IE elevation)



4 References

Bontemps, S. Defourny, P. Van Bogaert, E. Arino, O. Kalogirou, V. Ramos Perez, J. 2011. GLOBCOVER 2009, Product and validation report. ESA, UCL

Cole, T. G., Ewel, K. C., and Devoe, N. N. Structure of mangrove trees and forests in micronesia. *Forest Ecology and Management*, 117(1):95–109, 1999.

Danielson, Jeffrey J., Sandra K. Poppenga, John C. Brock, Gayla A. Evans, Dean J. Tyler, Dean B. Gesch, Cindy A. Thatcher, and John A. Barras. 2016. “Topobathymetric Elevation Model Development Using a New Methodology: Coastal National Elevation Database.” *Journal of Coastal Research*, December, 75–89. doi:10.2112/SI76-008.

Farr, T., Rosen, P., Caro, E., Crippen, R., Duren, R., Hensley, S., Alsdorf, D. (2007). The shuttle radar topography mission. *Reviews of Geophysics*, 45(2005), 1–33. <http://doi.org/10.1029/2005RG000183.1>. **INTRODUCTION**

Giri C, Ochieng E, Tieszen LL, Zhu Z, Singh A, Loveland T, Masek J, Duke N (2011). Status and distribution of mangrove forests of the world using earth observation satellite data (version 1.3, updated by UNEP-WCMC). *Global Ecology and Biogeography* 20: 154-159. doi: [10.1111/j.1466-8238.2010.00584.x](http://doi.org/10.1111/j.1466-8238.2010.00584.x) . Data URL: <http://data.unep-wcmc.org/datasets/4>

Horstman, E. M., Dohmen-Janssen, C. M., Narra, P. M. F., van den Berg, N. J. F., Siemerink, M., & Hulscher, S. J. M. H. (2014). Wave attenuation in mangroves: A quantitative approach to field observations. *Coastal Engineering*, 94, 47–62. doi:10.1016/j.coastaleng.2014.08.005

Janssen, M.P.J. (2016). Flood hazard reduction by mangroves. MSc. Thesis Delft University of Technology.

Mazda, Y., Magi, M., Ikeda, Y., Kurokawa, T., & Asano, T. (2006). Wave reduction in a mangrove forest dominated by *Sonneratia* sp. *Wetlands Ecology and Management*, 14(4), 365–378. doi:10.1007/s11273-005-5388-0

Mendez, F. J., & Losada, I. J. (2004). An empirical model to estimate the propagation of random breaking and nonbreaking waves over vegetation fields. *Coastal Engineering*, 51(2), 103–118.

Möller, I., Kudella, M., Rupprecht, F., Spencer, T., Paul, M., van Wesenbeeck, B. K., Wolter, G., Jense, K., Bouma, T.J., Miranda-Lange, M., & Schimmels, S. (2014). Wave attenuation over coastal salt marshes under storm surge conditions. *Nature Geoscience*, 7(10), 727–731. <http://doi.org/10.1038/ngeo2251> doi:10.1016/j.coastaleng.2003.11.003

Muis, S., Verlaan, M., Winsemius, H. C., Aerts, J. C. J. H., & Ward, P. J. (2016). A global reanalysis of storm surges and extreme sea levels. *Nature Communications*, 7, 11969. doi:10.1038/ncomms11969



- Narayan, S., Beck, M. W., Reguero, B. G., Losada, I. J., van Wesenbeeck, B., Pontee, N., ... Burks-Copes, K. A. (2016). The Effectiveness, Costs and Coastal Protection Benefits of Natural and Nature-Based Defences. *PLoS One*, 11(5), e0154735. doi:10.1371/journal.pone.0154735
- Pullen, T., Allsop, N. W. H., Bruce, T., Kortenhuis, A., Schüttrumpf, H., & Van der Meer, J. W. (2007). *EurOtop, European Overtopping Manual - Wave overtopping of sea defences and related structures: Assessment manual*.
- Songy, G.M. (2016). *Wave attenuation by global coastal salt marsh habitats*. MSc. Thesis Delft University of Technology.
- Van Rooijen, A. A., McCall, R. T., van Thiel de Vries, J. S. M., van Dongeren, A. R., Reniers, A. J. H. M., & Roelvink, J. A. (2016). Modeling the effect of wave-vegetation interaction on wave setup. *Journal of Geophysical Research: Oceans*. doi:10.1002/2015JC011392
- Vuik, V., Jonkman, S. N., Borsje, B. W., Suzuki, T., Kratzer, I., & Bouma, T. J. (2015). Nature-based flood protection: the efficiency of vegetated foreshores in reducing wave run-up. *Coastal Engineering*, 116, 42–56. doi:10.1016/j.coastaleng.2016.06.001
- Wiegmann, N., Perluka, R., Oude Elberink, S., Vogelzang, J., 2005. *Vaklodingen: de inwintechnieken en hun combinaties. Vergelijking tussen verschillende inwintechnieken en de combinaties ervan. Rapportnr: AGI-2005-GSMH-012*
<http://www.vliz.be/imisdocs/publications/112037.pdf>
- Zhu et al. (2012). Continuous monitoring of forest disturbance using all available Landsat imagery. *Remote Sensing of Environment*. Volume 122, July 2012, Pages 75–91. <http://www.sciencedirect.com/science/article/pii/S0034425712000387>



Annex I: Example metadata files

Global mean Intertidal elevation

Global mean intertidal elevation in meters above mean sea level for the period 1997 to 2017

This data set contains rasters where each pixel represents a floating point value of time-averaged (1997 - 2017) surface elevation (m, relative to MSL) in the inter-tidal zone (between LAT and HAT). The product was derived from the NASA/USGS Landsat and EU/ESA/Copernicus Sentinel 2 earth observation collections combined with CNES-AVISO+ Global tide - FES2012 tidal simulations. The product was produced as tiles for areas-of-interest covering the majority of the global coastline, with all available images selected between 1997 and 2017, however because of differences in the number of images available and quality filtering some tiles do not have coverage and temporal bias varies per tile. The same issue occurs in terms of nominal spatial resolution, which ranges from 20 to 30 m for the Sentinel 2 and Landsat sensors. Estimation of the accuracy of elevation estimations at 6 European case study sites (salt marsh and tidal flat systems) gave a mean absolute error of < 1 m. Artifacts are often observed in volcanic, mountainous, urban and snow affected regions. We recommend using the product as a guide to inter-tidal elevation and carrying out calibrations whenever possible. This data is not suitable for any purpose involving human safety. The research leading to these results was carried within the framework of the project Foreshore Assessment Using Space Technology (FAST), which received funding from the European Union Seventh Framework Programme (FP7/2007-2013) under grant agreement n° 607131. All views presented are those of the author's, the European Union is not liable for any use that may be made of the information contained therein.

Download and links Help with Download

Google Earth Derived Intertidal elevation
http://al-tc004.xtr.deltares.nl:8080/geoserver/FAST_global_imagery/wms?service=WMS&version=1.1.0&request=GetMap&layers=FAST_global_imagery:GEE_intertidal_elevation&styles=&bbox=-7.000027,-7.456

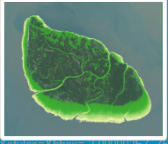
Type **dataset**

Quality Unknown

Time Extent From 1996-12-31 until 2016-12-31

Keywords

Show all metadata
Email feedback



Global yes/no vegetation

Global Yes/No Vegetation Maps for the period 2013 to 2017

This data set contains rasters where each pixel represents a yes/no vegetation (2013 - 2017). The product was derived from the NASA/USGS Landsat 8 and EU/ESA/Copernicus Sentinel 2 earth observation collections combined. The product was produced as tiles for areas-of-interest covering the majority of the global coastline, with all available images selected between 2013 and 2017, however because of differences in the number of images available and quality filtering some tiles do not have coverage and temporal bias varies per tile. The same issue occurs in terms of nominal spatial resolution, which ranges from 20 to 30 m for the Sentinel 2 and Landsat sensors. We recommend using the product as a guide to yes/no and carrying out calibrations whenever possible. This data is not suitable for any purpose involving human safety. The research leading to these results was carried within the framework of the project Foreshore Assessment Using Space Technology (FAST), which received funding from the European Union Seventh Framework Programme (FP7/2007-2013) under grant agreement n° 607131. All views presented are those of the author's, the European Union is not liable for any use that may be made of the information contained therein.

Download and links Help with Download

Global Yes/No vegetation map
http://al-tc004.xtr.deltares.nl:8080/geoserver/FAST_global_imagery/wms?service=WMS&version=1.1.0&request=GetMap&layers=FAST_global_imagery:GEE_vegetation&styles=&bbox=-7.000027,-7.456

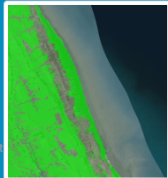
Type **dataset**

Quality Unknown

Time Extent From 1996-12-31 until 2016-12-31

Keywords

Show all metadata
Email feedback



Global change of vegetation

Global Vegetation change

Global vegetation change estimates are provided globally as GeoTIFF files with three bands and UINT16 pixel depth. Folder names indicate the region of the Earth to which the contents relate. Estimates are based on difference between vegetation presence/absence maps derived for the periods 16/07/1984-16/07/1989 and 01/01/2013-15/12/2016 using Google Earth Engine script Global_Veg_Change20.js. Mean NDVI and seasonal NDVI fluctuation amplitude thresholds used for determination of presence/absence = 0.20. Bands: Band 1: Change estimate - 0= NoData, 1= Vegetation present in both times, 2= Vegetation loss, 3=Vegetation gain Band 2: Number of images used to estimate presence/absence of vegetation in 1984-1989 time period Band 3: Number of images used to estimate presence/absence of vegetation in 2013-2016 time period

Download and links Help with Download

Vegetation change Europe (Google Earth Engine derived change in vegetation)
http://fast.openearth.nl/geoserver/FAST_global_imagery/wms?service=WMS&version=1.1.0&request=GetMap&layers=FAST_global_imagery:Vegetation%20ChangeEurope&styles=&bbox=-7.000027,-7.456

FAST Repository with source (login required)
https://repos.deltares.nl/repos/FAST/Global/spac-e/Global_Veg_Change_GEE

Type **dataset**

Quality Not Validated

Time Extent From 1983-12-31 until 2016-12-30

Keywords

- vegetation
- Google Earth Engine
- europe
- change
- Europe
- Boundaries

Show all metadata
Email feedback





This project has received funding from the European Union's Seventh Framework Programme for research, technological development and demonstration under grant agreement n° 607131.

Grant Agreement number: 607131
 DG Research - FP7 - SPACE - 2013

EMODnet Bathymetry CADIZ (detailed form)

Details

WHAT?

Data set name/coverage	DTM OF THE COASTAL REGION OF CÁDIZ
Discipline	Marine geology Terrestrial
Parameter groups	Gravity, magnetics and bathymetry Terrestrial
Discovery parameters	Bathymetry and Elevation
GEMET-INSPIRE themes	Oceanographic geographical features
Abstract	MULTI BEAM DATA OBTAINED WITH EM300/GEOSWATH 500 ECHOSOUNDERS AND GPS DIFFERENTIAL POSITIONING SYSTEM. THE SURVEY AREA IS APPROACHES OF PORT OF CÁDIZ AND WESTERN OF ESTRECHO DE GIBRALTAR IN CÁDIZ PROVINCE
Data format	Climate and Forecast NetCDF Version 3.5
Data set creation date	20140618

WHERE?

Map



Name	Description
bnd_ATSCADM_1	Boundary
bnd_ATSCADM_2	Boundary
bnd_ATSCADM_3	Boundary

GML id	ms01
Datum	World Geodetic System 84
Measuring area type	surface
Water depth (m)	-9999
Depth reference	Lowest Astronomical Tide
Minimum instrument depth (m)	44.66
Maximum instrument depth (m)	197.15
Sea regions	Northeast Atlantic Ocean (40W) Strait of Gibraltar

WHEN?

Start date	20040929
Start time	00:00:00
End date	20050614
End time	00:00:00
Temporal resolution	1 Seconds

HOW?

Instrument / gear type	multi-beam echosounders
Horizontal resolution	1 Metres
Vertical resolution	2.7 Metres
Platform type	naval vessel
Cruise name	TOFIÑO
Alternative cruise name	TOFIÑO
Cruise start date	20040929

WHO?

Originator	Hydrographic Institute of the Navy
Data Holding centre	Hydrographic Institute of the Navy

HOW TO GET THE DATA?

Data Distributor	Hydrographic Institute of the Navy
Access/ordering of data	web data access with registration
Access restriction	by negotiation

OTHER INFO

Name	Date	Comment
COMMISSION REGULATION (EC) No 1205/2008 of 3 December 2008 implementing Directive 2007/2/EC of the European Parliament and of the Council as regards metadata	2008-12-04	See the referenced specification

The data centres apply standard data quality control procedures on all data that the centres manage. Ask the data centre for details.

CDI-METADATA

CDI-record id	1982328
CDI-record creation date	20140319
CDI-record last update	20140620
CDI-partner	Hydrographic Institute of the Navy

The selected data set is described above with metadata. Access to the data set itself can be requested via the EMODnet Bathymetry portal that gives an overview and access to marine and ocean data sets acquired and managed by European organisations. Go to: <http://www.emodnet-bathymetry.eu>

All data are also available through the pan-European SeaDataNet portal <http://www.seadatanet.org>





This project has received funding from the European Union's Seventh Framework Programme for research, technological development and demonstration under grant agreement n° 607131.

Grant Agreement number: **607131**
DG Research - FP7 - SPACE - 2013